

# Flavor Physics in an SO(10) Grand Unified Model

JENNIFER GIRRBACH<sup>1</sup>, SEBASTIAN JÄGER<sup>2</sup>, MARKUS KNOPF<sup>1</sup>, WALDEMAR MARTENS<sup>1</sup>,  
ULRICH NIERSTE<sup>1</sup>, CHRISTIAN SCHERRER<sup>1</sup> AND SÖREN WIESENFELDT<sup>1,3</sup>

<sup>1</sup> *Institut für Theoretische Teilchenphysik  
Karlsruhe Institute of Technology  
Universität Karlsruhe  
Engesserstraße 7  
D-76128 Karlsruhe, Germany*

<sup>2</sup> *University of Sussex  
Department of Physics and Astronomy  
Falmer  
Brighton BN1 9QH  
United Kingdom*

<sup>3</sup> *Helmholtz Association, Anna-Louisa-Karsch-Str. 2, 10178 Berlin, Germany*

## Abstract

In supersymmetric grand-unified models, the lepton mixing matrix can possibly affect flavor-changing transitions in the quark sector. We present a detailed analysis of a model proposed by Chang, Masiero and Murayama, in which the near-maximal atmospheric neutrino mixing angle governs large new  $b \rightarrow s$  transitions. Relating the supersymmetric low-energy parameters to seven new parameters of this SO(10) GUT model, we perform a correlated study of several flavor-changing neutral current (FCNC) processes. We find the current bound on  $\mathcal{B}(\tau \rightarrow \mu\gamma)$  more constraining than  $\mathcal{B}(B \rightarrow X_s\gamma)$ . The LEP limit on the lightest Higgs boson mass implies an important lower bound on  $\tan\beta$ , which in turn limits the size of the new FCNC transitions. Remarkably, the combined analysis does not rule out large effects in  $B_s-\bar{B}_s$  mixing and we can easily accomodate the large CP phase in the  $B_s-\bar{B}_s$  system which has recently been inferred from a global analysis of CDF and DØ data. The model predicts a particle spectrum which is different from the popular Constrained Minimal Supersymmetric Standard Model (CMSSM).  $\mathcal{B}(\tau \rightarrow \mu\gamma)$  enforces heavy masses, typically above 1 TeV, for the sfermions of the degenerate first two generations. However, the ratio of the third-generation and first-generation sfermion masses is smaller than in the CMSSM and a (dominantly right-handed) stop with mass below 500 GeV is possible.

## 1 Introduction

Although the standard model (SM) is extremely successful, it is likely that it is only an effective theory, subsumed by a more fundamental theory at short distances. Weak-scale supersymmetry (SUSY) supplies a means to stabilize a hierarchy between the electroweak and more fundamental

scales. Remarkably, with the renormalization group (RG) equations of the minimal supersymmetric extension of the standard model (MSSM) above the weak scale, the three gauge couplings meet at  $M_{\text{GUT}} = 2 \times 10^{16}$  GeV [1]. This supports the idea that the strong, weak, and electromagnetic interactions are unified into a grand unified theory (GUT) with a single gauge coupling [2, 3]. It is striking that the experimental evidence for small but non-vanishing neutrino masses fits nicely in this framework, as  $M_{\text{GUT}}$  is of the right order of magnitude to generate small Majorana masses for the neutrinos.

SO(10) [4] is arguably the most natural GUT group: both the SM gauge and matter fields are unified, introducing only one additional matter particle, the right-handed neutrino. It is an anomaly-free theory and therefore explains the intricate cancellation of the anomalies in the standard model [5]. Moreover, it contains  $B - L$  as a local symmetry, where  $B$  and  $L$  are baryon and lepton number, respectively; the breaking of  $B - L$  naturally provides light neutrino masses via the seesaw mechanism [6].

Despite its theoretical attractiveness, the experimental hints for supersymmetric GUTs have been sparse, putting stringent constraints on models. In particular, the impressive agreement of the flavor precision measurements with the standard model leads to the widespread belief that the Yukawa couplings are the only source of flavor violation; this concept is known as minimal flavor violation [7].

In the (supersymmetric) standard model, fermion mixing is only measurable among the left-handed states and described by the quark and lepton mixing matrices,  $V_{\text{CKM}}$  and  $U_{\text{PMNS}}$ . The mixing angles of  $V_{\text{CKM}}$  are small, corresponding to the strong mass hierarchy, while two angles in  $U_{\text{PMNS}}$  turn out to be large. These are the neutrino solar and atmospheric mixing angles, where the latter is close to maximal,  $\theta_{23} \simeq \left(42.3^{+5.1}_{-3.3}\right)^\circ$  at  $1\sigma$  [8]. The definition of minimal flavor violation in Ref. [7] involves independent flavor symmetry groups for quarks and leptons. It confines the effects of  $V_{\text{CKM}}$  to the quark sector and that of  $U_{\text{PMNS}}$  to the lepton sector. In GUTs, however, this separation of quark and lepton sector is abrogated as quarks and leptons are unified and thus their masses and mixing are related to each other. While different patterns are possible, it is natural to expect imprints of  $U_{\text{PMNS}}$  on the quark sector as well. For instance, the Yukawa couplings (and thus the masses) of down quarks and charged leptons unify in SU(5) with [3]

$$Y_d = Y_e^\top. \quad (1)$$

This relation indicates that one might encounter small rotations between left-handed down quarks and right-handed leptons in connection with large mixing among right-handed down quarks and left-handed leptons. The mixing of the right-handed fermions is unobservable due to the absence of right-handed currents at the weak scale. With weak-scale supersymmetry, however, the mixing of the corresponding scalar partners of quarks and leptons becomes physical. Hence, one might ask whether the large mixing angles are observable in the quark sector [9–13]<sup>1</sup>.

The concept of minimal flavor violation suggests the assumption that the supersymmetry breaking parameters are universal at some scale. This ansatz is realized in the minimal supergravity (mSUGRA) scenario [15] (or a popular variant of it, the CMSSM [16]), where the scale, at which the relations hold, is usually taken to be  $M_{\text{GUT}}$ . FCNC processes in this framework have been

<sup>1</sup>For an earlier study with  $V_{\text{CKM}}$  being the universal mixing matrix, see Ref. [14].

calculated already 20 years ago [17]. A more natural choice for high-scale supersymmetry breaking, however, is to impose flavor universality at the Planck scale,  $M_{\text{Pl}} = G_N^{-1/2} = 1 \cdot 10^{19}$  GeV.<sup>2</sup> The reason to take  $M_{\text{GUT}}$  instead of  $M_{\text{Pl}}$  is simply that while the use of the renormalization group equations of the MSSM below  $M_{\text{GUT}}$  is undisputed, the analysis of the region between  $M_{\text{GUT}}$  and  $M_{\text{Pl}}$  requires knowledge about the grand-unified model. The errors made in neglecting these effects are proportional to a loop suppression factor times  $\ln(M_{\text{Pl}}/M_{\text{GUT}})$ ; however, since the evolution of the parameters from  $M_{\text{GUT}}$  down to low energies breaks the universality of the SUSY breaking parameters, new effects in FCNC processes occur, as we will analyze in this paper.

Now, in the LHC era, it is desirable to have a predictive theory framework which links the results of a decade of precision flavor physics to quantities probed in high- $p_T$  collider physics, such as the masses of superpartners. The mSUGRA and CMSSM models minimize flavor effects in an ad-hoc way and lead to an MFV version in the sense of Ref. [7] of the MSSM. The purpose of this paper is to establish a well-motivated alternative scenario to the widely-studied MFV variants of the MSSM. We consider an SO(10) model laid out by Chang, Masiero and Murayama (CMM model) [12], which amounts to a version of the MSSM with a well-controlled source of new flavor violation linking the atmospheric neutrino mixing angle to transitions between right-handed  $b$  and  $s$  quarks. We perform a correlated analysis of several flavor-changing processes in the quark and lepton sector. This analysis involves seven parameters in addition to the parameters of the standard model (SM). Since the same parameters enter observables studied in the high- $p_T$  programs of CMS and ATLAS, the CMM model may serve as a benchmark model connecting quark and lepton flavor physics to collider physics. As a first step in this direction we study the masses of superpartners and of the lightest neutral Higgs boson. In view of the rich Higgs sector of GUTs we emphasize a particular advantage of probing these with flavor physics: While flavor physics observables probe the Yukawa interactions between the Higgs and matter supermultiplets, they only depend very weakly on the poorly known parameters of the Higgs potential.

Prior to this paper no exhaustive RG analysis of the CMM model has been published. A CMM-inspired study has addressed the important topic of  $b \rightarrow s$  penguin amplitudes: In Ref. [18] the MFV-MSSM was complemented by a flavor-changing  $\tilde{b}_R - \tilde{s}_R$  term in the right-handed down-squark mass matrix, without implementing GUT relations among the MSSM parameters. This study was triggered by an experimental anomaly in the combined data of mixing-induced CP asymmetries in  $b \rightarrow s$  penguin amplitudes, which pointed to a discrepancy with the SM value inferred from the mixing-induced CP asymmetry measured in the tree-level decay  $B_d \rightarrow J/\psi K_S$ . Since the new  $b \rightarrow s$  transition of the CMM model involves right-handed quarks, the sign of the deviations of the CP asymmetries from their SM values should depend on the parity of the final state (*Kagan's theorem* [19, 20]), unless the new contribution dominates over the SM amplitude [21]. A first study relating MSSM to GUT parameters was performed in 2003 [22], showing that in the CMM model the —at that time unknown—  $B_s - \bar{B}_s$  oscillation frequency can exceed its SM value by up to a factor of 5. Then B-factory data seemed to show that the mixing-induced CP asymmetries in  $b \rightarrow s$  penguin amplitudes are, irrespectively of the parity of the final state, consistently lower than the SM value: The naive average of the CP asymmetries was reported to lie below the SM expectation

---

<sup>2</sup>Alternatively, one might choose the *reduced* Planck scale,  $M_{\text{Pl}} = (8\pi G_N)^{-1/2} = 2 \cdot 10^{18}$  GeV, because it compensates for the factor  $8\pi$  in the Einstein field equations.

by  $3.8\sigma$  in winter 2005 [23] and the interest in the CMM idea faded. Today's situation, however, is again favorable for the CMM model: CDF and DØ find the  $B_s - \bar{B}_s$  mixing oscillation frequency in agreement with the SM [24], which still leaves the possibility of roughly 50% corrections from new physics because of large hadronic uncertainties. The same experiments, however, find hints for a new CP-violating phase in  $B_s - \bar{B}_s$  mixing [25–30], which might imply a complex correction to the  $B_s - \bar{B}_s$  mixing amplitude of roughly half the size of the SM contribution. While the popular MFV scenarios of the MSSM cannot provide this correction, even if flavor-diagonal parameters (such as  $A_t$ ) are taken complex [31], this situation is covered by the range found for the CMM model in Ref. [22]. On the other hand the significance of the experimental anomalies in  $b \rightarrow s$  penguin amplitudes is steadily shrinking and current data do not challenge the SM much [32, 33]. The observed pattern of possible new  $\mathcal{O}(1)$  effects in  $B_s - \bar{B}_s$  mixing and small corrections to  $b \rightarrow s$  penguin amplitudes below the current experimental sensitivity is natural in the CMM model, as we discuss below.

The paper is organized as follows: In the next section we specify the theoretical framework of the CMM model focusing on its peculiarities in the flavor sector. In section 3 we describe the RGE analysis for the determination of the soft breaking parameters at the weak scale, followed by a presentation of observables that have been used to constrain the model in section 4. Finally, before concluding, we present our results in section 5 and compare our study with other analyses in section 6.

## 2 Framework

In this section we describe the CMM model and fill in some details which were not specified in Ref. [12].  $\text{SO}(10)$  is successively broken to  $\text{SU}(3)_C \times \text{U}(1)_{\text{em}}$  as

$$\text{SO}(10) \xrightarrow{\langle 16_H \rangle, \langle \bar{16}_H \rangle, \langle 45_H \rangle} \text{SU}(5) \xrightarrow{\langle 45_H \rangle} \text{G}_{\text{SM}} \equiv \text{SU}(3)_C \times \text{SU}(2)_L \times \text{U}(1)_Y \xrightarrow{\langle 10_H \rangle, \langle 10'_H \rangle} \text{SU}(3)_C \times \text{U}(1)_{\text{em}}. \quad (2)$$

The first breaking occurs at  $M_{\text{SO}(10)} \sim 10^{17}$  GeV, while the  $\text{SU}(5)$ -symmetry is broken at the MSSM unification scale,  $M_{\text{GUT}}$ . Actually, both the  $\text{SU}(5)$  singlet  $S$  and adjoint  $\Sigma_{24}$  of  $45_H$  have non-vanishing vevs: While the vev of the  $\text{SU}(5)$  adjoint,  $\langle \Sigma_{24}(45_H) \rangle \equiv \sigma$ , breaks  $\text{SU}(5)$  to the standard model group, the singlet component acquires a vev, when  $\text{SO}(10)$  is broken,  $\langle S(45_H) \rangle \equiv v_0$ . This latter vev will become important for the Yukawa couplings discussed below. The pair of spinors,  $16_H + \bar{16}_H$ , breaks the  $\text{U}(1)_{B-L}$  subgroup of  $\text{SO}(10)$ , reducing the rank of the group from five to four. With this setup, we restrict ourselves to small Higgs multiplets, where the threshold corrections at the various breaking scales are small and which allows for a perturbative  $\text{SO}(10)$  gauge coupling at the Planck scale  $M_{\text{Pl}}$ .<sup>3</sup>

<sup>3</sup>A complete model requires a suitable Higgs superpotential, both to achieve the pattern of VEVs assumed here and to give GUT-scale masses to all components in  $10_H, 10'_H, 45_H$  but for the two MSSM doublets (see below). The Higgs potential was not specified in [12], and we do not address this problem here. Rather, our focus in this paper is on the consequences of the breaking pattern and flavor structure on low-energy phenomenology. We feel our findings, in turn, motivate further work on the symmetry breaking dynamics, possibly along the lines of [34], which discusses a somewhat similar Higgs sector.

The three generations of standard model matter fields are unified into three spinorial representations, together with three right-handed neutrinos,

$$16_i = (Q, u^c, d^c, L, e^c, \nu^c)_i, \quad i = 1, 2, 3. \quad (3)$$

Here  $Q$  and  $L$  denote the quark and lepton doublet superfields and  $u^c$ ,  $d^c$ ,  $e^c$ , and  $\nu^c$  the corresponding singlet fields of the up and down antiquark as well as the positron and the antineutrino, respectively.

The Yukawa superpotential reads

$$W_Y = \frac{1}{2} 16_i Y_1^{ij} 16_j 10_H + 16_i Y_2^{ij} 16_j \frac{45_H 10'_H}{2 M_{\text{Pl}}} + 16_i Y_N^{ij} 16_j \frac{\overline{16}_H \overline{16}_H}{2 M_{\text{Pl}}}. \quad (4)$$

Let us discuss the individual terms in detail. The MSSM Higgs doublets  $H_u$  and  $H_d$  are contained in  $10_H$  and  $10'_H$ , respectively. Only the up-type Higgs doublet  $H_u$  in  $10_H$ , acquires a weak-scale vev such that the first term gives masses to the up quarks and neutrinos only. The masses for the down quarks and charged fermions are then generated through the vev of the down-type Higgs doublet of a second Higgs field  $H_d$  in  $10'_H$ . (A second Higgs field is generally needed in order to have a non-trivial CKM matrix.) They are obtained from the second term in Eq. (4) which is of mass-dimension five. In fact, this operator stands for various, nonequivalent effective operators with both the SU(5)-singlet and the SU(5)-adjoint vevs of the adjoint Higgs field such that the coupling matrix  $Y_2$  can only be understood symbolically. The operator can be constructed in various ways, for example by integrating out SO(10) fields at the Planck scale. The corresponding couplings can be symmetric or antisymmetric [35, 36], resulting in an asymmetric *effective* coupling matrix  $Y_2$ , as opposed to the symmetric matrices  $Y_1$  and  $Y_N$ . This asymmetric matrix allows for significantly different rotation matrices for the left and right-handed fields. For more details see Appendix A. The dimension-five coupling also triggers a natural hierarchy between the up and down-type quarks, corresponding to small values of  $\tan \beta$ , where  $\tan \beta$  is the ratio of the vacuum expectation values (vevs),  $\tan \beta = \langle H_u \rangle / \langle H_d \rangle$ . Finally, the third term in Eq. (4), again a higher-dimensional operator, generates Majorana masses for the right-handed neutrinos.

The Yukawa matrices are diagonalized as

$$\begin{aligned} Y_1 &= L_1 D_1 L_1^\top, \\ Y_2 &= L_2 D_2 R_2^\dagger, \\ Y_N &= R_N D_N P_N R_N^\top, \end{aligned} \quad (5)$$

where  $L_i$  and  $R_i$  are unitary matrices,  $P_N$  is a phase matrix, and  $D_{1,2,N}$  are diagonal with positive entries. In order to work out the physically observable mixing parameters, we choose the first coupling to be diagonal, i.e., we transform the matter field as  $16 \rightarrow L_1^* 16$  such that

$$W_Y = \frac{1}{2} 16^\top D_1 16 10_H + 16^\top L_1^\dagger L_2 D_2 R_2^\dagger L_1^* 16 \frac{45_H 10'_H}{2 M_{\text{Pl}}} + 16^\top L_1^\dagger R_N D_N P_N R_N^\top L_1^* 16 \frac{\overline{16}_H \overline{16}_H}{2 M_{\text{Pl}}}. \quad (6)$$

Since the up-quarks have diagonal couplings, either of the  $Y_2$  mixing matrices,  $L_1^\dagger L_2$  or  $R_2^\dagger L_1^*$ , must

describe the quark mixing. We will work in the SU(5) basis, in which the Yukawa couplings read

$$\begin{aligned}
W_Y = & \left[ \frac{1}{4} \Psi^\top D_1 \Psi + N^\top D_1 \Phi \right] H + \sqrt{2} \Psi^\top L_1^\dagger L_2 D_2' R_2^\dagger L_1^* \Phi H' \\
& + \frac{M_N}{2} N^\top L_1^\dagger R_N D_N P_N R_N^\top L_1^* N, \\
D_2' = & D_2 \frac{v_0}{M_{\text{Pl}}} , \quad M_N = \frac{\langle \overline{16}_H \rangle \langle \overline{16}_H \rangle}{M_{\text{Pl}}}
\end{aligned} \tag{7}$$

Here, we denote the SU(5) matter fields by  $\Psi_i = (Q_i, u_i^c, e_i^c)$ ,  $\Phi_i = (d_i^c, L_i)$  and  $N_i = \nu_i^c$  and the SU(5) Higgs fields by  $H = (H_u, *)$  and  $H' = (*, H_d)$ . The color-triplets in  $H$  and  $H'$  which acquire masses of order  $M_{\text{GUT}}$  are denoted by  $*$ . The vev  $v_0$  is defined after Eq. (2). Now we identify the quark mixing matrix as

$$V_q = L_1^\top L_2^*. \tag{8}$$

( $V_q$  coincides with the SM quark mixing matrix  $V_{\text{CKM}}$  up to phases.) We can always choose a basis where one of the three Yukawa matrices is diagonal. In the CMM model, however, one assumes that  $Y_1$  and  $Y_N$  are simultaneously diagonalizable, i.e.

$$L_1^\dagger R_N = \mathbb{1}. \tag{9}$$

This assumption is motivated by the observed values for the fermion masses and mixings and might be a result of family symmetries. First, we note that the up-quarks are more strongly hierarchical than the down quarks, charged leptons, and neutrinos. As a result, the eigenvalues of  $Y_N$  must almost have a double hierarchy, compared to  $Y_1$ . Then, given the Yukawa couplings in an arbitrary basis, we expect smaller off-diagonal entries in  $L_1$  than in  $L_2$  because hierarchical masses generically correspond to small mixing. Moreover, the light neutrino mass matrix implies that, barring cancellations, the rotations in  $L_1$  should rather be smaller than those in  $V_{\text{CKM}}$  [37]. Hence, even if the relation (9) does not hold exactly, the off-diagonal entries in  $L_1^\dagger R_N$  will be much smaller than the entries in  $V_{\text{CKM}}$  and they cannot spoil the large effects generated by the lepton mixing matrix,  $U_{\text{PMNS}}$ .

Our assumption that  $Y_1$  and  $Y_N$  are simultaneously diagonalizable permits an arbitrary phase matrix on the right-hand side of Eq. (9). However, this phase matrix can be absorbed into  $P_N$  introduced earlier in Eq. (5) (where this matrix could have been absorbed into  $R_N$ ). Now, with  $Y_1$  and  $Y_N$  being simultaneously diagonal, the flavor structure is (apart from supersymmetry breaking terms, which we will discuss below) fully contained in the remaining coupling,  $Y_2$ , and Eq. (6) simply reads

$$W_Y = \frac{1}{2} 16^\top D_1 16 10_H + 16^\top V_q^* D_2 R_2^\dagger L_1^* 16 \frac{45_H 10'_H}{2 M_{\text{Pl}}} + 16^\top D_N P_N 16 \frac{\overline{16}_H \overline{16}_H}{2 M_{\text{Pl}}}. \tag{10}$$

It is clear that this coupling has to account for both the quark and lepton mixing. Hence,  $Y_2$  cannot be symmetric.

As mentioned above, the higher-dimensional operator can be generated in various ways, generically resulting in the asymmetric effective coupling matrix  $Y_2$ . The dominant contributions come

from the singlet vev,  $v_0 \sim M_{\text{SO}(10)}$ , which is an order of magnitude higher than  $\sigma \sim M_{\text{GUT}}$ . In this case, the contributions are approximately the same for down quarks and charged leptons; a more detailed discussion is given in Appendix A. Then we can identify the lepton mixing matrix as

$$U_D = P_N^* R_2^\dagger L_1^* . \quad (11)$$

Again,  $U_D$  coincides with the lepton mixing matrix  $U_{\text{PMNS}}^*$  up to phases. In this paper, the Majorana phases contained in  $P_N$  are irrelevant and can therefore be neglected. We can then express the Yukawa coupling of the down quarks and charged leptons as

$$Y_2 = V_q^* D_2 U_D . \quad (12)$$

The relation (12) holds in the CMM model as long as we concentrate on the heaviest generation, namely the bottom quarks and the tau lepton. The masses of the lighter generations do not unify, so the higher-dimensional operators must partially contribute differently to down quarks and charged leptons (see Appendix A). Now one might wonder whether these corrections significantly modify the relation (12); however, the approximate bottom-tau unification and the good agreement between the SM predictions and the experimental data for  $B_d - \bar{B}_d$  mixing,  $\Delta M_K$  and  $\epsilon_K$  severely constrain these potential modification, as discussed in Ref. [38]. A corresponding analysis in the lepton sector (in a wider SU(5) framework) exploiting  $\mu \rightarrow e\gamma$  can be found in Ref. [39]. We can therefore safely neglect corrections to Eq. (12).

In terms of MSSM fields, the couplings simply read

$$\begin{aligned} W_Y = & Q_i D_1^{ij} u_j^c H_u + Q_i (V_q^* D_2' U_D)^{ij} d_j^c H_d \\ & + L_i D_1^{ij} \nu_j^c H_u + L_i (U_D^\top D_2' V_q^\dagger)^{ij} e_j^c H_d + \frac{1}{2} \nu_i^c D_N^{ij} \nu_j^c . \end{aligned} \quad (13)$$

Here  $Q_i D_1^{ij} u_j^c H_u$  is short-hand for  $\epsilon_{mn} Q_i^{\alpha m} D_1^{ij} u_{\alpha j}^c H_u^n$  with the SU(3)<sub>C</sub> and SU(2)<sub>L</sub> indices  $\alpha = 1, 2, 3$  and  $m, n = 1, 2$ , respectively, and similarly for the other couplings. Eq. (13) holds for exact SO(10) symmetry; below  $M_{\text{SO}(10)}$  the Yukawa couplings  $D_1^{ij}$  in the first and third terms will be different, as well as those in the second and fourth term.

Both  $V_q$  and  $U_D$  are unitary matrices, which generically have nine parameters each, namely three mixing angles and six phases. In the SM, we can eliminate five of the six phases in  $V_{\text{CKM}}$  by making phase rotations of the quark fields. Due to the Majorana nature of the neutrinos, we are left with three phases in  $U_{\text{PMNS}}$ . In the CMM model, however, we cannot rotate the quark and lepton fields separately without violating the implicit GUT constraint. Once we eliminate all but one phase in  $V_q$ , we are left with the full set of phases in  $U_D$ . To see the additional phases explicitly, let us write down the mixing matrix for the tri-bimaximal solution, corresponding to  $\theta_{12} = \arcsin(1/\sqrt{3}) \simeq 35^\circ$ ,  $\theta_{13} = 0^\circ$ , and  $\theta_{23} = 45^\circ$ ,

$$U_D^{\text{TBM}} = \Theta_L U_{\text{PMNS}}^{\text{TBM}*} \Theta_R = \begin{pmatrix} \sqrt{\frac{2}{3}} e^{-ia_1} & \frac{1}{\sqrt{3}} e^{-ia_2} & 0 \\ -\frac{1}{\sqrt{6}} e^{-ia_4} & \frac{1}{\sqrt{3}} e^{-i(-a_1+a_2+a_4)} & \frac{1}{\sqrt{2}} e^{-i(-a_1+a_3+a_4)} \\ \frac{1}{\sqrt{6}} e^{-ia_5} & -\frac{1}{\sqrt{3}} e^{-i(-a_1+a_2+a_5)} & \frac{1}{\sqrt{2}} e^{-i(-a_1+a_3+a_5)} \end{pmatrix} . \quad (14)$$

The sixth phase (the ‘standard’ phase  $\delta$ ) drops out due to  $\theta_{13} = 0^\circ$ . In Eq. (14), we choose a parametrization, where the phases could be absorbed via the phase matrices

$$\Theta_L = \text{diag}(e^{-ia_1}, e^{-ia_4}, e^{-ia_5}), \quad \Theta_R = \text{diag}(1, e^{i(a_1-a_2)}, e^{i(a_1-a_3)}), \quad U_D = \Theta_L U_{\text{PMNS}}^* \Theta_R. \quad (15)$$

acting on the fields on the left and right, respectively. However, we only have this freedom for either  $V_q$  or  $U_D$ . We choose  $V_q \equiv V_{\text{CKM}}$  to be in its standard parametrization, so  $U_D$  will have the structure indicated in Eq. (14). These phases are important constituents of our observables (see Section 4). If we restrict to transitions between the second and third generation as in  $B_s$ – $\bar{B}_s$  mixing then only one phase (difference) enters the observables. Then we can write<sup>4</sup>

$$U_D = \text{diag}(1, e^{i\xi}, 1) U_{\text{PMNS}}^*, \quad \xi = a_5 - a_4. \quad (16)$$

Let us now add the supersymmetry breaking terms,

$$\begin{aligned} \mathcal{L}_{\text{soft}} = & -\tilde{16}_i^* \mathbf{m}_{\tilde{16}}^{2ij} \tilde{16}_j - m_{10_H}^2 10_H^* 10_H - m_{10'_H}^2 10_H'^* 10_{H'} \\ & - m_{\tilde{16}_H}^2 \tilde{16}_H^* \tilde{16}_H - m_{\tilde{16}_H}^2 16_H^* 16_H - m_{45_H}^2 45_H^* 45_H \\ & - \left( \frac{1}{2} \tilde{16}_i \mathbf{A}_1^{ij} \tilde{16}_j 10_H + \tilde{16}_i \mathbf{A}_2^{ij} \tilde{16}_j \frac{45_H 10_{H'}}{2 M_{\text{Pl}}} + \tilde{16}_i \mathbf{A}_N^{ij} \tilde{16}_j \frac{\tilde{16}_H \tilde{16}_H}{2 M_{\text{Pl}}} + \text{h.c.} \right), \end{aligned} \quad (17)$$

where  $\mathbf{m}$  are the soft scalar mass matrices and  $\mathbf{A}_i$  the (dimensionful) coefficients of the scalar trilinear couplings. In addition, there are  $B$ -terms for the Higgs fields as well as gaugino mass terms. As discussed above, we assume universal parameters at  $M_{\text{Pl}}$ ,

$$m_{\tilde{16}_i}^2 = m_0^2 \mathbb{1}, \quad m_{10_H}^2 = m_{10'_H}^2 = m_{\tilde{16}_H}^2 = m_{\tilde{16}_H}^2 = m_{45_H}^2 = m_0^2, \quad (18a)$$

$$\mathbf{A}_1 = a_0 \mathbf{Y}_1, \quad \mathbf{A}_2 = a_0 \mathbf{Y}_2, \quad \mathbf{A}_N = a_0 \mathbf{Y}_N, \quad (18b)$$

as well as one universal gaugino mass,  $m_{\tilde{g}}$ . Thus at  $M_{\text{Pl}}$ , the soft masses are diagonal in any flavor basis. At lower energies, this universality is broken. In particular, it is broken at  $M_{\text{GUT}}$ , which leads to a different phenomenology than the CMSSM [16] or mSUGRA [17]. The renormalization group evolution is conveniently performed in a flavor basis in which the up-type Yukawa couplings are diagonal (up basis).

For completeness we also give the soft breaking terms for the CMM model in terms of SU(5) fields:

$$\begin{aligned} \mathcal{L}_{\text{soft}} = & -\tilde{\Psi}_i^* \mathbf{m}_{\tilde{\Psi}}^{2ij} \tilde{\Psi}_j - \tilde{\Phi}_i^* \mathbf{m}_{\tilde{\Phi}}^{2ij} \tilde{\Phi}_j - \left[ \frac{1}{2} \tilde{N}_i \mathbf{m}_{\tilde{N}}^{2ij} \tilde{N}_j + \text{h.c.} \right] \\ & - m_H^2 H^* H - m_{H'}^2 H'^* H' - m_{24_H}^2 24_H^* 24_H \\ & - \left[ \left( \frac{1}{4} \tilde{\Psi}^\top \mathbf{A}_1 \tilde{\Psi} + \tilde{N}^\top \mathbf{A}_N \tilde{N} \right) H + \sqrt{2} \tilde{\Psi}^\top \mathbf{A}_2 \tilde{\Phi} H' + \frac{M_N}{2} \tilde{N}^\top \mathbf{A}_N \tilde{N} + \text{h.c.} \right]. \end{aligned} \quad (19)$$

The fields  $\Psi_i$ ,  $\Phi_i$ ,  $N_i$ ,  $H$  and  $H'$  live in the representations 10,  $\bar{5}$ , 1, 5 and  $\bar{5}$  of SU(5), respectively.

<sup>4</sup>The corrections to the diagonalization matrix of the right-handed down quarks,  $U_D$ , are studied in [38].



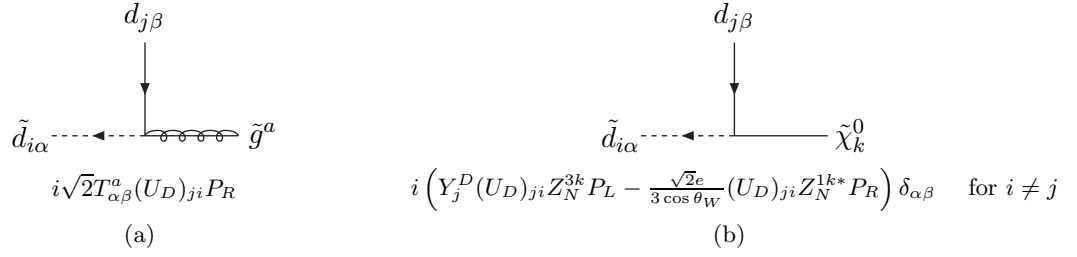


Figure 1: Quark-squark-gluino and quark-squark-neutralino vertices for  $i, j = 2, 3$ . Here  $d_{j\beta}$  is the Dirac field of the down-quark mass eigenstate of the  $j$ -th generation.  $\tilde{d}_{i\alpha}$  is the  $i$ -th-generation right-handed down-squark mass eigenstate (coinciding with the interaction eigenstate in the basis with  $\mathbf{Y}_1 = \mathbf{D}_1$ ).

In leading order, the soft mass matrix for the right-handed down squarks,  $\mathbf{m}_d^2$ , keeps its diagonal form but the third generation gets significant corrections from the large top Yukawa coupling, which are parametrized by the real parameter  $\Delta_{\tilde{d}}$ ,

$$\mathbf{m}_d^2(M_Z) = \text{diag}\left(m_d^2, m_{\tilde{d}}^2, m_d^2 - \Delta_{\tilde{d}}\right). \quad (20)$$

Here and in the following, the small Yukawa couplings of the first two generations are set to zero in the renormalization group equations. Now choosing the super-CKM basis<sup>5</sup> where the down quarks are mass eigenstates, this matrix is no longer diagonal,

$$\mathbf{m}_D^2 = U_D \mathbf{m}_d^2 U_D^\dagger = \begin{pmatrix} m_d^2 & 0 & 0 \\ 0 & m_d^2 - \frac{1}{2}\Delta_{\tilde{d}} & -\frac{1}{2}\Delta_{\tilde{d}}e^{i\xi} \\ 0 & -\frac{1}{2}\Delta_{\tilde{d}}e^{-i\xi} & m_d^2 - \frac{1}{2}\Delta_{\tilde{d}} \end{pmatrix}, \quad \xi \equiv a_5 - a_4, \quad (21)$$

allowing flavor-changing quark-squark-gluino and quark-squark-neutralino vertices (Fig. 1). Similarly, we get for the sleptons  $\mathbf{m}_L^2 = U_D \mathbf{m}_l^2 U_D^\dagger$ . The CP phase<sup>6</sup>  $\xi$  is of utmost importance for the phenomenology of  $b \rightarrow s$  transitions. It is worthwhile to compare the situation at hand with the usual MSSM with generic flavor structure: In the latter model all off-diagonal elements of the squark mass matrices are ad-hoc complex parameters, constrained only by the hermiticity of the squark mass matrices. In the CMM model, the phase factor  $e^{i\xi}$  originates from the Yukawa matrix  $\mathbf{Y}_2$  in Eq. (12) and enters Eq. (21) through a rotation of right-handed superfields.

Similarly, relation (18b) holds at the Planck scale. Running the MSSM trilinear terms  $\mathbf{A}_d$  and  $\mathbf{A}_e$  down to the electroweak scale, off-diagonal entries appear in the super-CKM basis due to the large mixing matrix  $U_D$ . These entries yield additional flavor violating effects. The running of the parameters in the various regions will be discussed in the following section. In our notation, we denote trilinear breaking terms that are defined in the super-CKM basis by a hat (e.g.  $\hat{\mathbf{A}}_d$ ).

Let us finally discuss two important aspects of the analysis which originate from the model's group structure. One, when the  $\text{SU}(5)$  singlet component of the spinorial Higgs field,  $16_H$ , acquires

<sup>5</sup>For the soft-terms and rotation matrices we will always use the convention of [40]

<sup>6</sup>In [38] the phase  $\xi$  corresponds to  $\phi_{B_s}$  in absence of Yukawa corrections to the first two generations. Note that in [38] a different convention for the soft terms of  $\tilde{d}^c, \tilde{u}^c, \tilde{e}^c$  is used:  $\tilde{d}^c \mathbf{m}_d^2 \tilde{d}^{c*}$  and not  $\tilde{d}^{c*} \mathbf{m}_d^2 \tilde{d}^c$  such that  $\mathbf{m}_d^2 = (\mathbf{m}_d^2)^* [38]$ .

a vev,  $\text{SO}(10)$  is not broken to its maximal subgroup  $\text{SU}(5) \times \text{U}(1)_X$  (where  $X = 5(B - L) - 4Y$ ) but to  $\text{SU}(5)$ . The  $\text{SO}(10)$  spinor decomposes as  $16 \rightarrow 10_1 + \bar{5}_{-3} + 1_5$  with respect to  $\text{SU}(5) \times \text{U}(1)_X$ , so we see that the  $\text{SU}(5)$  singlet has a non-trivial  $\text{U}(1)_X$  charge. Acquiring its vev, it breaks  $\text{U}(1)_X$  and reduces the rank of the group from five to four. Now, because of this rank reduction, additional D-term contributions to the soft masses appear, which are associated with the spontaneously broken diagonal generator of  $\text{U}(1)_X$  [41]. They are proportional to the  $\text{U}(1)_X$  charge of the  $\text{SU}(5)$ -fields but do not depend on the precise form of the  $\text{U}(1)_X$  breaking superpotential, nor on the scale where it is broken. In contrast, they depend on the soft masses and are of the same size as the other SUSY breaking terms, even though the scale of the  $\text{U}(1)_X$  breaking is many orders of magnitude larger. Hence, these contributions can be thought of as corrections to the relations (18a).

The  $\text{SO}(10)$  vector field decomposes as  $10 \rightarrow 5_{-2} + \bar{5}_2$  with respect to  $\text{SU}(5) \times \text{U}(1)_X$ . Hence, the soft masses of the  $\text{SU}(5)$  fields are given by

$$\begin{aligned} m_{\Psi_i}^2(t_{\text{SO}(10)}) &= m_{16_i}^2(t_{\text{SO}(10)}) + D, & m_H^2(t_{\text{SO}(10)}) &= m_{10_H}^2(t_{\text{SO}(10)}) - 2D, \\ m_{\Phi_i}^2(t_{\text{SO}(10)}) &= m_{16_i}^2(t_{\text{SO}(10)}) - 3D, & m_{H'}^2(t_{\text{SO}(10)}) &= m_{10_{H'}}^2(t_{\text{SO}(10)}) + 2D, \\ m_{N_i}^2(t_{\text{SO}(10)}) &= m_{16_i}^2(t_{\text{SO}(10)}) + 5D, \end{aligned} \quad (22)$$

where  $D$  denotes the additional D-term contribution and  $t = \ln \mu_r$  with the renormalization scale  $\mu_r$ .  $D$  is another parameter which enters our analysis when we relate weak scale observables to universal parameters at  $M_{\text{Pl}}$ . Since  $D$  affects all fermion generations in the same way, its effect on flavor physics is small.

Two, we have to check whether the fields of the unbroken subgroups are properly normalized. Decomposing the vector and adjoint of  $\text{SO}(10)$  in  $\text{SU}(5)$  representations, we see that both the fundamental and adjoint  $\text{SU}(5)$ -fields need to be rescaled by a factor of  $\sqrt{2}$  [42]. In order to have a continuous gauge coupling, however, we should instead rescale the  $\text{SO}(10)$  generators by a factor  $1/\sqrt{2}$ ,

$$T_{ij} = \frac{1}{\sqrt{2}} \mathcal{T}_{ij}, \quad (23)$$

where  $\mathcal{T}_{ij}$  are the  $\text{SO}(10)$  generators in the usual normalization, satisfying

$$(\mathcal{T}_{ij})_{mn} = i(\delta_{im}\delta_{jn} - \delta_{in}\delta_{jm}), \quad [\mathcal{T}_{ij}, \mathcal{T}_{kl}] = i(\delta_{jk}\mathcal{T}_{il} - \delta_{il}\mathcal{T}_{jk} - \delta_{jl}\mathcal{T}_{ik} + \delta_{ik}\mathcal{T}_{jl}). \quad (24)$$

At the same time, this redefinition of the  $\text{SO}(10)$  generators avoids a rescaling of the top Yukawa coupling by a factor  $\sqrt{2}$  [43].

In summary, the CMM model is a simple but well-motivated  $\text{SO}(10)$  model, which allows for large mixing among right-handed down quarks and therefore interesting effects in flavor changing processes. Actually, these effects are a consequence of the underlying GUT structure (evident in the relation  $Y_d = Y_e^\top$ ), the large top coupling and weak-scale supersymmetry. Compared to the SM, we have only a small number of additional parameters affecting the low-energy physics we plan to study: So far we have encountered the SUSY breaking parameters  $m_0$ ,  $m_{\tilde{g}}$  and  $a_0$ , the D-term correction  $D$  and the CP phase  $\xi$ . We will need two more parameters,  $\tan \beta$  and the phase of the Higgs mass parameter  $\mu$ .

This small set of parameters makes the model very predictive.

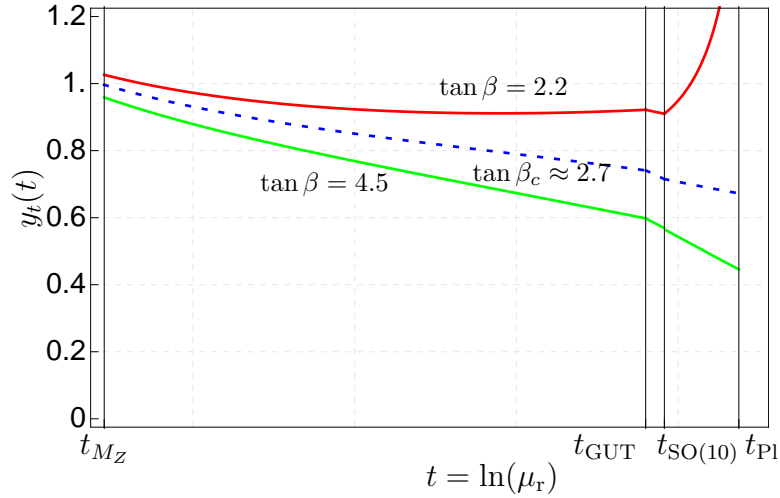


Figure 2: If  $\tan \beta$  is too small,  $y_t$  becomes non-perturbative below the Planck scale. The dotted line corresponds to a value of  $\tan \beta$ , where  $g/y_t$  reaches its fixed point at  $t_{\text{SO}(10)}$ . The kinks in the functions are due to the change of the gauge group.

### 3 Renormalization Group Equations

#### 3.1 Top Yukawa Coupling and its Infrared Fixed Point

For small values of  $\tan \beta$ , the top Yukawa  $y_t$  coupling is of order unity. In this case, the coupling can become non-perturbative below the Planck scale, in particular in GUT scenarios which generically include larger representations than the MSSM. The  $\text{SO}(10)$  RGE for the gauge and top Yukawa coupling have an infrared quasi-fixed point at one loop for  $g^2/y_t^2 = 56/55$  [44–46]. Thus, for larger values of  $y_t$  at  $M_{\text{SO}(10)}$ , its value may become non-perturbative below the Planck scale. In the CMM model the main driver of the FCNC effects is the RG revolution between  $M_{\text{P_I}}$  and  $M_{\text{SO}(10)}$ . Therefore, with increasing  $\tan \beta$  the model specific  $b \rightarrow s$  transitions quickly die out.

In the CMM model, the infrared fixed point corresponds to  $\tan \beta \simeq 2.7$  as one can see in Fig. 2. Our analysis will be located close to this fixed point, hence a precise knowledge of  $y_t$  is important. For this reason we will use the two-loop RGE in the MSSM. The default values in our analysis are  $\tan \beta = 3$  and  $\tan \beta = 6$ .

#### 3.2 Threshold correction and conversion to $\overline{\text{DR}}$ Scheme

We use the two-loop RG equations for the gauge and Yukawa couplings in the  $\overline{\text{DR}}$  scheme with one-loop SUSY threshold corrections at the electroweak scale [47, 48]. The reason for NLO accuracy here is the delicate dependence of the FCNC effects on  $y_t(M_Z)$  shown in Fig. 2. For scheme consistency the one-loop threshold corrections must be included with two-loop RGEs. Above  $t_{\text{GUT}}$  one-loop accuracy is sufficient. In the MSSM we use the approximated formula from Ref. [48] that include only potentially large corrections. For simplicity the decoupling scale is set to  $M_Z$ . The initial

values for the gauge couplings  $\tilde{\alpha}_i \equiv \alpha_i/(4\pi)$  are then given as

$$\begin{aligned}\tilde{\alpha}_1(M_Z) &= \frac{5}{3} \frac{\alpha_e(M_Z)}{4\pi \cos^2 \theta_W}, \\ \tilde{\alpha}_2(M_Z) &= \frac{\alpha_e(M_Z)}{4\pi \sin^2 \theta_W}, \\ \tilde{\alpha}_3(M_Z) &= \frac{1}{4\pi} \frac{\alpha_s(M_Z)}{1 - \Delta\alpha_s}, \quad \Delta\alpha_s = \frac{\alpha_s(M_Z)}{2\pi} \left[ \frac{1}{2} - \frac{2}{3} \ln \frac{m_t}{M_Z} - 2 \ln \frac{m_{\tilde{g}_3}}{M_Z} - \frac{1}{6} \sum_{i=1}^{12} \ln \frac{M_{\tilde{q}_i}}{M_Z} \right],\end{aligned}\tag{25}$$

where stands  $M_{\tilde{q}_i}$  for the mass eigenvalues of the 12 up and down squarks and  $m_{\tilde{g}_3}$  is the gluino mass. Here and in the following a tilde on a quantity always means that it has been divided by  $4\pi$ .

For the Yukawa couplings, we take both complex SUSY parameters and large off-diagonal elements in  $m_d^2$  and  $A_d$  into account. Then the top Yukawa coupling including threshold corrections is given by

$$\begin{aligned}\tilde{y}_t(M_Z) &= \frac{m_t}{4\pi v \sin \beta \left(1 + \frac{\Delta m_t}{m_t}\right)}, \\ \frac{\Delta m_t}{m_t} &= \tilde{\alpha}_3(M_Z) \left[ 4 \ln \frac{M_Z^2}{m_t^2} + \frac{20}{3} - \frac{4}{3} (B_1(0, m_{\tilde{g}_3}, m_{\tilde{t}_1}) + B_1(0, m_{\tilde{g}_3}, m_{\tilde{t}_2})) \right. \\ &\quad \left. + \frac{4}{3} e^{i\delta_{\tilde{t}}} \sin(2\theta_{\tilde{t}}) \frac{m_{\tilde{g}_3}}{m_t} (B_0(0, m_{\tilde{g}_3}, m_{\tilde{t}_1}) - B_0(0, m_{\tilde{g}_3}, m_{\tilde{t}_2})) \right],\end{aligned}\tag{26}$$

where  $\theta_{\tilde{t}}$  and  $\delta_{\tilde{t}}$  denote the stop mixing parameters defined later in this paragraph. The electroweak vev is denoted as  $v = \sqrt{\langle H_u \rangle^2 + \langle H_d \rangle^2} \approx 174$  GeV. The loop functions  $B_0$  and  $B_1$  are given as follows:

$$B_0(0, m_1, m_2) = -\ln \frac{M^2}{M_Z^2} + 1 + \frac{m^2}{m^2 - M^2} \ln \frac{M^2}{m^2},\tag{27a}$$

$$B_1(0, m_1, m_2) = \frac{1}{2} \left[ -\ln \frac{M^2}{M_Z^2} + \frac{1}{2} + \frac{1}{1-x} + \frac{\ln x}{(1-x)^2} - \theta(1-x) \ln x \right],\tag{27b}$$

with  $M = \max(m_1, m_2)$ ,  $m = \min(m_1, m_2)$ , and  $x = m_2^2/m_1^2$ .

The corrections for the bottom coupling are slightly more involved. We include these corrections

to account for CP phases. In the end, however, they turn out to be not relevant for small  $\tan \beta$ .

$$\begin{aligned} \tilde{y}_b(M_Z) &= -\frac{\hat{m}_b^{\text{SM}}(M_Z)}{4\pi v \cos \beta \left(1 + \frac{\Delta m_b}{m_b}\right)}, \\ \frac{\Delta m_b}{m_b} &= \left(\frac{\Delta m_b}{m_b}\right)^{\tilde{t}\tilde{\chi}^+} + \left(\frac{\Delta m_b}{m_b}\right)^{\tilde{b}\tilde{g}_3}, \\ \left(\frac{\Delta m_b}{m_b}\right)^{\tilde{t}\tilde{\chi}^+} &= \tilde{y}_t \mu^* \frac{\tilde{A}_t^* \tan \beta + \mu \tilde{y}_t}{m_{\tilde{t}_1}^2 - m_{\tilde{t}_2}^2} [B_0(0, |\mu|, m_{\tilde{t}_1}) - B_0(0, |\mu|, m_{\tilde{t}_2})] \\ &\quad - \tilde{\alpha}_2 \frac{\mu^* m_{\tilde{g}_2} \tan \beta}{|\mu|^2 - m_{\tilde{g}_2}^2} [\cos^2 \theta_{\tilde{t}} B_0(0, m_{\tilde{g}_2}, m_{\tilde{t}_1}) + \sin^2 \theta_{\tilde{t}} B_0(0, m_{\tilde{g}_2}, m_{\tilde{t}_2}) \\ &\quad - \cos^2 \theta_{\tilde{t}} B_0(0, |\mu|, m_{\tilde{t}_1}) - \sin^2 \theta_{\tilde{t}} B_0(0, |\mu|, m_{\tilde{t}_2})], \\ \left(\frac{\Delta m_b}{m_b}\right)^{\tilde{b}\tilde{g}_3} &= -\frac{4}{3} \tilde{\alpha}_3(M_Z) \left[ B_1(0, m_{\tilde{g}_3}, m_{\tilde{b}_1}) + B_1(0, m_{\tilde{g}_3}, m_{\tilde{b}_2}) - 2 \frac{m_{\tilde{g}_3}}{m_b} \sum_{i=1}^6 Z_D^{6i*} Z_D^{3i} B_0(0, m_{\tilde{g}_3}, m_{\tilde{d}_i}) \right]. \end{aligned} \quad (28)$$

with  $\hat{m}_b^{\text{SM}}(M_Z) = 2.92$  GeV. The matrix  $Z_D$  is the  $6 \times 6$  mixing matrix for the down squarks defined in Ref. [40];  $m_t$  UN  $m_b$  denote the pole masses of the top and bottom quarks, respectively; and the loop functions are given in Eqs. (27).  $\tilde{A}_t$  is the  $(3, 3)$  entry of the trilinear soft breaking term for the up squarks.  $\mu$  is the SUSY Higgs parameter and  $m_{\tilde{t}_i}$ ,  $m_{\tilde{b}_i}$  are the eigenvalues of the stop and sbottom mass matrix. Furthermore, we denote the mass of the  $\text{SU}(2)_L$  gaugino by  $m_{\tilde{g}_2}$ . Finally, the initial condition for the tau coupling reads

$$\tilde{y}_\tau(M_Z) = -\frac{m_\tau}{4\pi v \cos \beta}. \quad (29)$$

The  $2 \times 2$  mass matrix of the scalar top quarks,

$$\mathcal{M}_t^2 = \begin{pmatrix} m_{\tilde{q}_3}^2 + m_t^2 + \left(\frac{1}{2} - \frac{2}{3} \sin^2 \theta_W\right) M_Z^2 \cos(2\beta) & -m_t \left(\frac{\tilde{A}_t}{\tilde{y}_t} + \frac{\mu^*}{\tan \beta}\right) \\ -m_t \left(\frac{\tilde{A}_t^*}{\tilde{y}_t} + \frac{\mu}{\tan \beta}\right) & m_{\tilde{u}_3}^2 + m_t^2 + \frac{2}{3} \sin^2 \theta_W M_Z^2 \cos(2\beta) \end{pmatrix}, \quad (30)$$

is diagonalized by the unitary matrix  $\tilde{Z}_U^T$ ,

$$\tilde{Z}_U^T \mathcal{M}_t^2 \tilde{Z}_U^* = \begin{pmatrix} m_{\tilde{t}_1}^2 & 0 \\ 0 & m_{\tilde{t}_2}^2 \end{pmatrix}, \quad \tilde{Z}_U^T = \begin{pmatrix} \cos \theta_{\tilde{t}} & e^{i\delta_{\tilde{t}}} \sin \theta_{\tilde{t}} \\ -e^{-i\delta_{\tilde{t}}} \sin \theta_{\tilde{t}} & \cos \theta_{\tilde{t}} \end{pmatrix}, \quad (31)$$

which is the  $(3, 6)$ -submatrix of  $Z_U^T$ , the analogon of  $Z_D^T$  for the up squarks [40]. The mixing angle and phase are computed via

$$\tan \theta_{\tilde{t}} = \frac{2m_t \left| \frac{\tilde{A}_t}{\tilde{y}_t} + \frac{\mu^*}{\tan \beta} \right|}{m_{\tilde{q}_3}^2 - m_{\tilde{u}_3}^2 + \left(\frac{1}{2} - \frac{4}{3} \sin^2 \theta_W\right) M_Z^2 \cos(2\beta)}, \quad \delta_{\tilde{t}} = \arg \left[ -m_t \left( \frac{\tilde{A}_t}{\tilde{y}_t} + \frac{\mu^*}{\tan \beta} \right) \right], \quad (32)$$

where the  $(3, 3)$  elements of the (diagonal) soft breaking masses have been denoted by  $m_{\tilde{u}_3}^2$  and  $m_{\tilde{q}_3}^2$ . Note that we do not include threshold corrections in the mixing matrices, because they appear only in expressions that are of one-loop order already. The resulting effect would be one more order higher, which can safely be neglected.

### 3.3 Gauge and Yukawa Couplings

As discussed above, we use the two-loop RGEs in the MSSM. They can be found in Ref. [47] and are listed in our notation below. We do not include Higgs self-interactions in the RGEs because we do not specify the couplings of the Higgs superfields to each other. Qualitatively they would not change the outcome of our analysis since Higgs self-interactions are always flavor blind. Including them would only lead to an absolute shift in the allowed parameter space of the model. We neglect both the small Yukawa couplings of the lighter generations as well as the CKM matrix, as its flavor violating entries are small compared to those in  $U_D$ . Here and in the following,  $t = \ln \mu_\tau$ , where  $\mu_\tau$  is the renormalization scale.

$$\frac{d}{dt} \tilde{\alpha}_1 = 2\tilde{\alpha}_1^2 \left( \frac{33}{5} + \frac{199}{25} \tilde{\alpha}_1 + \frac{27}{5} \tilde{\alpha}_2 + \frac{88}{5} \tilde{\alpha}_3 - \frac{26}{5} |\tilde{y}_t|^2 - \frac{14}{5} |\tilde{y}_b|^2 - \frac{18}{5} |\tilde{y}_\tau|^2 \right) \quad (33)$$

$$\frac{d}{dt} \tilde{\alpha}_2 = 2\tilde{\alpha}_2^2 \left( 1 + \frac{9}{5} \tilde{\alpha}_1 + 25\tilde{\alpha}_2 + 24\tilde{\alpha}_3 - 6 |\tilde{y}_t|^2 - 6 |\tilde{y}_b|^2 - 2 |\tilde{y}_\tau|^2 \right) \quad (34)$$

$$\frac{d}{dt} \tilde{\alpha}_3 = 2\tilde{\alpha}_3^2 \left( -3 + \frac{11}{5} \tilde{\alpha}_1 + 9\tilde{\alpha}_2 + 14\tilde{\alpha}_3 - 4 |\tilde{y}_t|^2 - 4 |\tilde{y}_b|^2 \right) \quad (35)$$

$$\begin{aligned} \frac{d}{dt} \tilde{y}_t &= \tilde{y}_t \left( 6 |\tilde{y}_t|^2 + |\tilde{y}_b|^2 - \frac{16}{3} \tilde{\alpha}_3 - 3\tilde{\alpha}_2 - \frac{13}{15} \tilde{\alpha}_1 \right) \\ &\quad + \tilde{y}_t \left( -22 |\tilde{y}_t|^4 - 5 |\tilde{y}_b|^4 - 5 |\tilde{y}_b \tilde{y}_t|^2 - |\tilde{y}_b \tilde{y}_\tau|^2 \right. \\ &\quad \left. + 16\tilde{\alpha}_3 |\tilde{y}_t|^2 + \frac{6}{5} \tilde{\alpha}_1 |\tilde{y}_t|^2 + 6\tilde{\alpha}_2 |\tilde{y}_t|^2 + \frac{2}{5} \tilde{\alpha}_1 |\tilde{y}_b|^2 \right. \\ &\quad \left. - \frac{16}{9} \tilde{\alpha}_3^2 + \frac{15}{2} \tilde{\alpha}_2^2 + \frac{2743}{450} \tilde{\alpha}_1^2 + 8\tilde{\alpha}_3 \tilde{\alpha}_2 + \frac{136}{45} \tilde{\alpha}_3 \tilde{\alpha}_1 + \tilde{\alpha}_1 \tilde{\alpha}_2 \right) \end{aligned} \quad (36)$$

$$\begin{aligned} \frac{d}{dt} \tilde{y}_b &= \tilde{y}_b \left( 6 |\tilde{y}_b|^2 + |\tilde{y}_t|^2 + |\tilde{y}_\tau|^2 - \frac{16}{3} \tilde{\alpha}_3 - 3\tilde{\alpha}_2 - \frac{7}{15} \tilde{\alpha}_1 \right) \\ &\quad + \tilde{y}_b \left( -22 |\tilde{y}_b|^4 - 5 |\tilde{y}_t|^4 - 3 |\tilde{y}_\tau|^4 - 5 |\tilde{y}_b \tilde{y}_t|^2 - 3 |\tilde{y}_b \tilde{y}_\tau|^2 \right. \\ &\quad \left. + 16\tilde{\alpha}_3 |\tilde{y}_b|^2 + \frac{2}{5} \tilde{\alpha}_1 |\tilde{y}_b|^2 + 6\tilde{\alpha}_2 |\tilde{y}_b|^2 + \frac{6}{5} \tilde{\alpha}_1 |\tilde{y}_\tau|^2 + \frac{4}{5} \tilde{\alpha}_1 |\tilde{y}_t|^2 \right. \\ &\quad \left. + \frac{16}{9} \tilde{\alpha}_3^2 + \frac{15}{2} \tilde{\alpha}_2^2 + \frac{287}{90} \tilde{\alpha}_1^2 + 8\tilde{\alpha}_3 \tilde{\alpha}_2 + \frac{8}{9} \tilde{\alpha}_3 \tilde{\alpha}_1 + \tilde{\alpha}_1 \tilde{\alpha}_2 \right) \end{aligned} \quad (37)$$

$$\begin{aligned} \frac{d}{dt} \tilde{y}_\tau &= \tilde{y}_\tau \left( 4 |\tilde{y}_\tau|^2 + 3 |\tilde{y}_b|^2 - 3\tilde{\alpha}_2 - \frac{9}{5} \tilde{\alpha}_1 \right) \\ &\quad + \tilde{y}_\tau \left( -19 |\tilde{y}_\tau|^4 - 9 |\tilde{y}_\tau \tilde{y}_b|^2 - 3 |\tilde{y}_b \tilde{y}_t|^2 + 16\tilde{\alpha}_3 |\tilde{y}_b|^2 - \frac{2}{5} \tilde{\alpha}_1 |\tilde{y}_b|^2 \right. \\ &\quad \left. + \frac{6}{5} \tilde{\alpha}_1 |\tilde{y}_\tau|^2 + 6\tilde{\alpha}_2 |\tilde{y}_\tau|^2 + \frac{15}{2} \tilde{\alpha}_2^2 + \frac{9}{5} \tilde{\alpha}_1 \tilde{\alpha}_2 + \frac{27}{2} \tilde{\alpha}_1^2 \right) \end{aligned} \quad (38)$$

### SU(5)

At  $M_{\text{GUT}}$ , the gauge couplings unify. As is well known, this unification is not exact in the MSSM at the two-loop level but will be compensated by threshold effects, caused by the GUT particle

spectrum. Due to the larger uncertainties of the strong coupling, we use the criterion  $\tilde{\alpha}_1(t_{\text{GUT}}) = \tilde{\alpha}_2(t_{\text{GUT}}) \equiv \tilde{\alpha}$ . Similarly, we choose the bottom coupling as input for  $\mathbf{Y}_2$ .

The singlet neutrinos are integrated out at their mass scales, the heaviest of which is an order of magnitude smaller than  $M_{\text{GUT}}$ . However, we do not take the effect of the neutrino coupling  $\tilde{y}_{\nu_3}$  between  $M_{N_3}$  and  $M_{\text{GUT}}$  into account. At  $M_{\text{GUT}}$ , we identify  $\tilde{y}_{\nu_3} = \tilde{y}_t$  according to Eq. (13).

We use one-loop RGE as given in [49]. In our notation, they read

$$\frac{d}{dt}\tilde{\alpha} = -6\tilde{\alpha}^2, \quad (39)$$

$$\frac{d}{dt}\tilde{y}_t = \tilde{y}_t \left( -\frac{96}{5}\tilde{\alpha} + 9|\tilde{y}_t|^2 + 4|\tilde{y}_b|^2 + |\tilde{y}_{\nu_3}|^2 \right), \quad (40)$$

$$\frac{d}{dt}\tilde{y}_b = \tilde{y}_b \left( -\frac{84}{5}\tilde{\alpha} + 10|\tilde{y}_b|^2 + 3|\tilde{y}_t|^2 + |(U_D)_{33}|^2 |\tilde{y}_{\nu_3}|^2 \right), \quad (41)$$

$$\frac{d}{dt}\tilde{y}_{\nu_3} = \tilde{y}_{\nu_3} \left( -\frac{48}{5}\tilde{\alpha} + 7|\tilde{y}_{\nu_3}|^2 + 3|\tilde{y}_t|^2 + 4|(U_D)_{33}|^2 |\tilde{y}_b|^2 \right). \quad (42)$$

### SO(10)

The Yukawa couplings for the down quarks are generated via the non-renormalizable term. To derive its RGE, we generalize the equations from Ref. [47] to a dimension-five coupling. Here we make use of the non-renormalization theorem in supersymmetry, i.e. that only wave-function renormalization contributes to the beta functions. To verify that this theorem is applicable to the dimension-5 term at the one-loop level, note that each vertex diagram is equivalent to a vertex correction of a dimension-four interaction: E.g. diagrams in which the two matter supermultiplets are part of the loop are identical to the sum of corresponding diagrams with  $45_H 10'_H$  replaced by single Higgs superfields transforming as  $\underline{10}, \underline{120}, \dots$ . The RGE for  $\tilde{\mathbf{Y}}_2$  reads:

$$\frac{d}{dt}\tilde{\mathbf{Y}}_2 = -\frac{95}{2}\tilde{\alpha}\tilde{\mathbf{Y}}_2 + 10 \left( \tilde{\mathbf{Y}}_1 \tilde{\mathbf{Y}}_1^\dagger \tilde{\mathbf{Y}}_2 + \tilde{\mathbf{Y}}_2 \tilde{\mathbf{Y}}_1^\dagger \tilde{\mathbf{Y}}_1 \right), \quad (43)$$

where again  $\tilde{\alpha} = \alpha/(4\pi)$ ,  $\tilde{\mathbf{Y}}_i = \mathbf{Y}_i/(4\pi)$  and  $t = \ln \mu_r$ . In practice, however, we will only need the RGE for the bottom-coupling,

$$\frac{d}{dt}\tilde{y}_b = \tilde{y}_b \left( -\frac{95}{2}\tilde{\alpha} + 10 \left( 1 + |(U_D)_{33}|^2 \right) |\tilde{y}_t|^2 \right). \quad (44)$$

Note that  $\mathbf{Y}_2$  and  $\tilde{y}_b$  are the SO(10) couplings, which will be rescaled at the SO(10) breaking scale (see Eq. (13)), e.g.

$$\tilde{y}'_b(t_{\text{SO}(10)}) = \frac{v_0}{M_{\text{Pl}}} \tilde{y}_b(t_{\text{SO}(10)}), \quad (45)$$

where the prime denotes the SU(5) coupling. The prime, however, is omitted in our SU(5) RGEs.

The equations for the top coupling and the gauge coupling read

$$\frac{d}{dt}\tilde{y}_t = \tilde{y}_t \left( -\frac{63}{2}\tilde{\alpha} + 28|\tilde{y}_t|^2 \right) \quad (46)$$

$$\frac{d}{dt}\tilde{\alpha} = -8\tilde{\alpha}^2. \quad (47)$$

### 3.4 Supersymmetry Breaking Parameters

The soft masses and  $A$ -terms at the scale  $M_Z$  are fixed by the universal terms  $a_0$ ,  $m_0^2$ , and  $D$  through the renormalization group equations (RGE). Instead of guessing their values at  $M_{\text{Pl}}$ , we will consider three parameters at  $M_Z$  which are allowed by theoretical and experimental constraints. These are the soft masses of the first generation of right-handed up and down squarks and the (11)-element of the trilinear coupling of the down squarks,

$$m_{\tilde{u}_1}^2(M_Z), \quad m_{\tilde{d}_1}^2(M_Z), \quad a_1^d(M_Z) \equiv \left[ a^d(M_Z) \right]_{11}. \quad (48)$$

We work in the weak basis with diagonal  $\mathbf{Y}_1$  and the trilinear term  $a_1^d$  is defined with the corresponding Yukawa coupling factored out, in analogy to  $a_0$  in Eq. (18b). With these initial conditions we can evolve the soft terms up to  $M_{\text{GUT}}$ , where the MSSM fields are unified into the SU(5) multiplets  $\Phi$  and  $\Psi$  with

$$m_{\tilde{\Psi}_1}^2(t_{\text{GUT}}) = m_{\tilde{u}_1}^2(t_{\text{GUT}}), \quad m_{\tilde{\Phi}_1}^2(t_{\text{GUT}}) = m_{\tilde{d}_1}^2(t_{\text{GUT}}). \quad (49)$$

After running from  $M_{\text{GUT}}$  to  $M_{\text{SO}(10)}$  we can calculate  $D$  by means of Eqs. (22),

$$D = \frac{1}{4} \left[ m_{\tilde{\Psi}_1}^2(t_{\text{SO}(10)}) - m_{\tilde{\Phi}_1}^2(t_{\text{SO}(10)}) \right], \quad (50)$$

and determine

$$m_{\tilde{16}_1}^2(t_{\text{SO}(10)}) = \frac{1}{4} \left[ 3m_{\tilde{\Psi}_1}^2(t_{\text{SO}(10)}) + m_{\tilde{\Phi}_1}^2(t_{\text{SO}(10)}) \right]. \quad (51)$$

Then the universal scalar soft mass at the Planck scale is found:

$$m_0^2 = m_{\tilde{16}_1}^2(t_{\text{Pl}}) \quad (52)$$

The determination of the universal gaugino mass  $m_{\tilde{g}}$  is much simpler: At leading order the ratio  $\kappa \equiv m_{\tilde{g}_i}(t)/\tilde{\alpha}_i(t)$  is RG invariant, independent of  $i$  and equal to its SU(5) and SO(10) GUT values,  $\kappa = m_{\tilde{g}}(t)/\tilde{\alpha}(t)$  [47]. We determine  $\kappa$  from the gluino mass and the QCD coupling:

$$m_{\tilde{g}_i}(t) = \kappa \tilde{\alpha}_i(t), \quad (53)$$

where

$$\kappa \equiv \frac{m_{\tilde{g}_3}(M_Z)}{\tilde{\alpha}_3(M_Z)}. \quad (54)$$

The RGE needed to determine the Planck scale parameters are

$$\begin{aligned} \text{MSSM:} \quad & \frac{d}{dt} a_1^d = - \left( \frac{32}{3} \tilde{\alpha}_3^2 + 6 \tilde{\alpha}_2^2 + \frac{14}{15} \tilde{\alpha}_1^2 \right) \kappa \\ \text{SU(5):} \quad & \frac{d}{dt} a_1^d = - \frac{168}{5} \tilde{\alpha}^2 \kappa \\ \text{SO(10):} \quad & \frac{d}{dt} a_1^d = -95 \tilde{\alpha}^2 \kappa \quad \Rightarrow \quad a_0 = a_1^D(t_{\text{Planck}}) \end{aligned} \quad (55)$$



and

$$\begin{aligned}
\text{MSSM:} \quad & \frac{d}{dt} m_{\tilde{u}_1}^2 = -\frac{32}{3} \kappa^2 \tilde{\alpha}_3^3 - \frac{32}{15} \kappa^2 \tilde{\alpha}_1^3 - \frac{4}{5} \frac{S_{\text{GUT}}}{\tilde{\alpha}_{\text{GUT}}} \tilde{\alpha}_1^2 \\
& \frac{d}{dt} m_{\tilde{d}_1}^2 = -\frac{32}{3} \kappa^2 \tilde{\alpha}_3^3 - \frac{18}{15} \kappa^2 \tilde{\alpha}_1^3 + \frac{2}{5} \frac{S_{\text{GUT}}}{\tilde{\alpha}_{\text{GUT}}} \tilde{\alpha}_1^2 \\
\text{SU(5):} \quad & \frac{d}{dt} m_{\tilde{\Psi}_1}^2 = -\frac{144}{5} \kappa^2 \tilde{\alpha}^3 \\
& \frac{d}{dt} m_{\tilde{\Phi}_1}^2 = -\frac{96}{5} \kappa^2 \tilde{\alpha}^3 \\
\text{SO(10):} \quad & \frac{d}{dt} m_{\mathbf{16}_1}^2 = -45 \kappa^2 \tilde{\alpha}^3 \quad \Rightarrow \quad m_0^2 = m_{\mathbf{16}_1}^2(t_{\text{Planck}})
\end{aligned} \tag{56}$$

Here we have used the quantity

$$S_{\text{GUT}} \equiv m_{H_u}^2(t_{\text{GUT}}) - m_{H_d}^2(t_{\text{GUT}}) \tag{57}$$

which is defined in a more general way in Eq. (4.27) of [47]. We exploit the leading-order RG invariance of the ratio  $\frac{S}{\tilde{\alpha}_1} = \frac{S_{\text{GUT}}}{\tilde{\alpha}_{\text{GUT}}}$  to eliminate several soft masses from the RGE.

In summary, as inputs for the CMM model we need the soft masses of  $\tilde{u}_R$  and  $\tilde{d}_R$  of the first generations  $m_{\tilde{u}_1}^2$ ,  $m_{\tilde{d}_1}^2$  and  $a_1^d$ , the mass  $m_{\tilde{g}_3}$  as well as the phase of  $\mu$ . Additionally,  $\tan \beta$  and the phase  $\xi$  can be chosen as free input parameters, but  $\tan \beta$  cannot be large because of the bottom Yukawa coupling is suppressed by a factor of  $M_{\text{SO}(10)}/M_{\text{Pl}}$ . Initially, we set  $m_{\tilde{u}_1}^2 = m_{\tilde{d}_1}^2 = M_{\tilde{q}}$  at the weak scale and use a three-dimensional polynomial fit for the quantity  $S_{\text{GUT}}$ . This fit is computed by initially setting  $S_{\text{GUT}} = 0$  and obtaining well convergent values after two runs depending on the variables  $M_{\tilde{q}}(M_Z)$ ,  $a_1^d(M_Z)$  and  $m_{\tilde{g}_3}(M_Z)$ .

We run up to the Planck scale using the RGE and the unification conditions specified above. Then we evolve back from  $M_{\text{Pl}}$  through SO(10), SU(5) and the MSSM to the electroweak scale and determine the remaining relevant parameters like soft masses. We can further now determine the magnitude of the MSSM Higgs parameter  $\mu$  from the condition of electroweak symmetry breaking: With  $m_{H_u}^2$  and  $m_{H_d}^2$  from the first run we determine  $|\mu(M_Z)|$  using

$$|\mu| = \frac{m_{H_u}^2 \sin^2 \beta - m_{H_d}^2 \cos^2 \beta}{\cos(2\beta)} - \frac{1}{2} M_Z, \tag{58}$$

which is used as input for the second run of the RGE. The phase of  $\mu$  is left as a free input. With the first run also  $S_{\text{GUT}}/\tilde{\alpha}_{\text{GUT}}$  is determined anew. To stabilize our solution we repeat the RG evolution to the Planck scale and back with the input values refined through the first run. We find good convergence already after two complete runs.

The RGE for the soft SUSY-breaking terms of the first generation are given in Eqs. (55) and (56). The RGE governing the soft terms of the third generation that are needed for the running from the Planck scale back to the electroweak scale are more complicated because of the flavor mixing stemming from  $U_D$  and the involvement of  $\tilde{y}_t$ . These equations are listed and are discussed in the following Secs. 3.5 and 3.6.

### 3.5 RGE of trilinear terms

At the Planck scale we have

$$\tilde{\mathbf{A}}_1 = a_0 \tilde{\mathbf{Y}}_1, \quad \tilde{\mathbf{A}}_2 = a_0 \tilde{\mathbf{Y}}_2, \quad (59)$$

so that the trilinear terms are diagonal in the same basis as the Yukawa couplings. In our basis with diagonal  $\tilde{\mathbf{Y}}_1, \tilde{\mathbf{Y}}_u$  the matrix  $\tilde{\mathbf{A}}_1, \tilde{\mathbf{A}}_u$  stays diagonal down to the scale  $M_Z$ . It is therefore sufficient to consider  $\tilde{A}_t := (\tilde{\mathbf{A}}_u)_{33}$ . However, the large atmospheric mixing angle induces a non-negligible (3,2) element in  $\tilde{\mathbf{A}}_2, \tilde{\mathbf{A}}_d$  at  $M_Z$ . This corresponds to a non-negligible (2,3) element in  $\tilde{\mathbf{A}}_e$ .  $(\tilde{\mathbf{A}}_d)_{32}$  induces novel  $\tilde{b}_L \rightarrow \tilde{s}_R$  transitions.

#### SO(10)

The RGE for  $\tilde{A}_t = (\tilde{\mathbf{A}}_1)_{33}$  is easily obtained from [47]. We derive the RGE for  $\hat{\tilde{A}}_2$  in the same way as those for  $\hat{\tilde{Y}}_2$  in Eq. (43), by generalizing Eqs. (2.7)–(2.10) of [47]. The group factors are calculated in a straightforward way and can be found e.g. in [66]. The desired equations read

$$\begin{aligned} \frac{d}{dt} \tilde{A}_t &= -\frac{63}{2} \tilde{\alpha} \left( 2\tilde{\alpha} \kappa \tilde{y}_t + \tilde{A}_t \right) + 84 \tilde{A}_t |\tilde{y}_t|^2, \\ \frac{d}{dt} \hat{\tilde{A}}_2 &= -\frac{95}{2} \tilde{\alpha} \left( 2\tilde{\alpha} \kappa \hat{\tilde{Y}}_2 + \hat{\tilde{A}}_2 \right) \\ &\quad + 10 \left( \hat{\tilde{Y}}_1 \hat{\tilde{Y}}_1^\dagger \hat{\tilde{A}}_2 + \hat{\tilde{A}}_2 U_D \hat{\tilde{Y}}_1 \hat{\tilde{Y}}_1^\dagger U_D^\dagger + 2 \hat{\tilde{A}}_1 \hat{\tilde{Y}}_1^\dagger \hat{\tilde{Y}}_2 + 2 \hat{\tilde{Y}}_2 U_D \hat{\tilde{Y}}_1^\dagger \hat{\tilde{A}}_1 U_D^\dagger \right) \end{aligned} \quad (60)$$

#### SU(5)

Using the RGEs from [49] and the rescaling conditions at the SO(10) scale analogously to the Yukawa couplings, the relevant equations read

$$\hat{\tilde{A}}^\nu(t_{\text{SO}(10)}) = \hat{\tilde{A}}^U(t_{\text{SO}(10)}) , \quad (\hat{\tilde{A}}_2(t_{\text{SO}(10)}))_{\text{SU}(5)} = \frac{v_0}{M_{\text{Pl}}} (\hat{\tilde{A}}_2(t_{\text{SO}(10)}))_{\text{SO}(10)} \quad (61)$$

$$\begin{aligned} \frac{d}{dt} \tilde{A}_t &= -\frac{96}{5} \tilde{\alpha} \left( 2\tilde{\alpha} \kappa \tilde{y}_t + \tilde{A}_t \right) + 2\tilde{y}_t \left( \tilde{y}_{\nu_3}^* \tilde{A}_{\nu_3} + 4\tilde{y}_b^* \tilde{A}_b \right) \\ &\quad + \tilde{A}_t (27|\tilde{y}_t|^2 + |\tilde{y}_{\nu_3}|^2 + 3|\tilde{y}_b|^2) , \\ \frac{d}{dt} \hat{\tilde{A}}_2 &= -\frac{84}{5} \tilde{\alpha} \left( 2\tilde{\alpha} \kappa \hat{\tilde{Y}}_2 + \hat{\tilde{A}}_2 \right) + \left( 4|\tilde{y}_b|^2 + 10\hat{\tilde{Y}}_2 \hat{\tilde{Y}}_2^\dagger + 3\hat{\tilde{Y}}_1 \hat{\tilde{Y}}_1^\dagger \right) \hat{\tilde{A}}_2 \\ &\quad + 8\hat{\tilde{A}}_2 \hat{\tilde{Y}}_2^\dagger \hat{\tilde{Y}}_2 + \hat{\tilde{A}}_2 U_D \hat{\tilde{Y}}_\nu^\dagger \hat{\tilde{Y}}_\nu U_D^\dagger + 8\tilde{y}_b^* \tilde{A}_b \hat{\tilde{Y}}_2 \\ &\quad + 6\hat{\tilde{A}}_1 \hat{\tilde{Y}}_1^\dagger \hat{\tilde{Y}}_2 + 2\hat{\tilde{Y}}_2 U_D \hat{\tilde{Y}}_\nu^\dagger \hat{\tilde{A}}_1 U_D^\dagger , \\ \frac{d}{dt} \hat{\tilde{A}}_\nu &= -\frac{48}{5} \tilde{\alpha} \left( 2\tilde{\alpha} \kappa \hat{\tilde{Y}}_\nu + \hat{\tilde{A}}_\nu \right) + \left( 3|\tilde{y}_t|^2 + |\tilde{y}_{\nu_3}|^2 + 7\hat{\tilde{Y}}_\nu \hat{\tilde{Y}}_\nu^\dagger \right) \hat{\tilde{A}}_\nu \\ &\quad + 6\tilde{y}_t^* \tilde{A}_t \hat{\tilde{Y}}_\nu + 2\tilde{y}_{\nu_3}^* \tilde{A}_{\nu_3} \hat{\tilde{Y}}_\nu + 4\hat{\tilde{A}}^\nu U_D^\dagger \hat{\tilde{Y}}_2^\dagger \hat{\tilde{Y}}_2 U_D \\ &\quad + 11\hat{\tilde{A}}_\nu \hat{\tilde{Y}}_\nu^\dagger \hat{\tilde{Y}}_\nu + 8\hat{\tilde{Y}}_\nu U_D^\dagger \hat{\tilde{Y}}_2^\dagger \hat{\tilde{A}}_2 U_D \end{aligned} \quad (62)$$

Here again  $\tilde{A}_t$ ,  $\tilde{A}_b$  and  $\tilde{A}_{\nu_3}$  are the (33) entries of the matrices  $\hat{\tilde{A}}_1$ ,  $\hat{\tilde{A}}_2$  and  $\hat{\tilde{A}}_\nu$ .

### MSSM

We integrate out the righthanded neutrino at the GUT scale and use the RGEs from [47]. Furthermore, we employ the SU(5) relation  $\mathbf{A}_e(t_{\text{GUT}}) = (\mathbf{A}_d(t_{\text{GUT}}))^T$  and evolve the trilinear terms down to the scale  $M_Z$ .

$$\begin{aligned}
\frac{d}{dt}\tilde{A}_t &= \tilde{A}_t \left( 8|\tilde{y}_t|^2 + |\tilde{y}_b|^2 - \frac{16}{3}\tilde{\alpha}_3 - 3\tilde{\alpha}_2 - \frac{13}{15}\tilde{\alpha}_1 \right) \\
&\quad + \tilde{y}_t \left( 10\tilde{y}_t^* \tilde{A}_t + 2\tilde{y}_b^* \tilde{A}_b - \frac{32}{3}\tilde{\alpha}_3^2 \kappa - 6\tilde{\alpha}_2^2 \kappa - \frac{26}{15}\tilde{\alpha}_1^2 \kappa \right), \\
\frac{d}{dt}\hat{\tilde{A}}_d &= \left( 3|\tilde{y}_b|^2 + |\tilde{y}_\tau|^2 + 5\hat{\tilde{Y}}_d^* (\hat{\tilde{Y}}_d)^T + \hat{\tilde{Y}}_u^* (\hat{\tilde{Y}}_u)^T - \frac{16}{3}\tilde{\alpha}_3 - 3\tilde{\alpha}_2 - \frac{7}{15}\tilde{\alpha}_1 \right) \hat{\tilde{A}}_d \\
&\quad + \left( 6\tilde{y}_b^* \tilde{A}_b + 2\tilde{y}_\tau^* \tilde{A}_\tau + 4\hat{\tilde{A}}_d \hat{\tilde{Y}}_d^\dagger + 2\hat{\tilde{A}}_u \hat{\tilde{Y}}_u^\dagger - \frac{32}{3}\tilde{\alpha}_3^2 \kappa - 6\tilde{\alpha}_2^2 \kappa - \frac{14}{15}\tilde{\alpha}_1^2 \kappa \right) \hat{\tilde{Y}}_d, \\
\frac{d}{dt}\hat{\tilde{A}}_e &= \left( 3|\tilde{y}_b|^2 + |\tilde{y}_\tau|^2 + 5\hat{\tilde{Y}}_e^* (\hat{\tilde{Y}}_e)^T - 3\tilde{\alpha}_2 - \frac{9}{5}\tilde{\alpha}_1 \right) \hat{\tilde{A}}_e \\
&\quad + \left( 6\tilde{y}_b^* \tilde{A}_b + 2\tilde{y}_\tau^* \tilde{A}_\tau + 4\hat{\tilde{A}}_e \hat{\tilde{Y}}_e^\dagger - 6\tilde{\alpha}_2^2 \kappa - \frac{18}{10}\tilde{\alpha}_1^2 \kappa \right) \hat{\tilde{Y}}_e.
\end{aligned} \tag{63}$$

### 3.6 RGE for soft masses

Employing the universality conditions of Eq. (18a) at the Planck scale, the soft masses stay diagonal in the basis with diagonal  $\tilde{\mathbf{Y}}_u$ . We list the RGEs for the first and second generation (index 1) and the third generation (index 3), which is separates due to the large top Yukawa coupling.

### SO(10)

We use the RGE from appendix B.1 of [66].

$$\begin{aligned}
\frac{d}{dt}m_{161}^2 &= -45\kappa^2 \tilde{\alpha}^3, \\
\frac{d}{dt}m_{163}^2 &= -45\kappa^2 \tilde{\alpha}^3 + 20|\tilde{y}_t|^2 \left[ 2m_{163}^2 + m_{10}^2 \right] + 20|\tilde{A}_t|^2, \\
\frac{d}{dt}m_{10H}^2 &= -36\kappa^2 \tilde{\alpha}^3 + 16|\tilde{y}_t|^2 \left[ 2m_{163}^2 + m_{10}^2 \right] + 16|\tilde{A}_t|^2, \\
\frac{d}{dt}m_{10'H}^2 &= -36\kappa^2 \tilde{\alpha}^3.
\end{aligned} \tag{64}$$

## SU(5)

After taking into account the D-term splitting in Eq. (22), we evolve the soft masses down to the GUT scale using the RGEs from [49]. For the numerical solution we can safely set  $\tilde{y}_{\nu_3} = \tilde{y}_t$ .

$$\begin{aligned}
\frac{d}{dt}m_{\tilde{\Phi}_1}^2 &= -\frac{96}{5}\kappa^2\tilde{\alpha}^3 + 8(U_D^\dagger\hat{\tilde{A}}_2^\dagger\hat{\tilde{A}}_2U_D)_{11} \\
&\quad + 8|(U_D)_{31}|^2|\tilde{y}_b|^2 \left[ m_{\tilde{\Phi}_1}^2 + m_{H'}^2 + m_{\tilde{\Psi}_3}^2 \right], \\
\frac{d}{dt}m_{\tilde{\Phi}_3}^2 &= -\frac{96}{5}\kappa^2\tilde{\alpha}^3 + 8(U_D^\dagger\hat{\tilde{A}}_2^\dagger\hat{\tilde{A}}_2U_D)_{33} + 2|\tilde{A}_{\nu_3}|^2 + 2|\tilde{y}_{\nu_3}|^2 \left[ m_{\tilde{\Phi}_3}^2 + m_H^2 + m_{\tilde{N}_3}^2 \right] \\
&\quad + 8|(U_D)_{33}|^2|\tilde{y}_b|^2 \left[ m_{\tilde{\Phi}_3}^2 + m_{H'}^2 + m_{\tilde{\Psi}_3}^2 \right], \\
\frac{d}{dt}m_{\tilde{\Psi}_1}^2 &= -\frac{144}{5}\kappa^2\tilde{\alpha}^3, \\
\frac{d}{dt}m_{\tilde{\Psi}_3}^2 &= -\frac{144}{5}\kappa^2\tilde{\alpha}^3 + 4|\tilde{y}_b|^2 \left[ m_{\tilde{\Psi}_3}^2 + m_{H'}^2 + (U_D m_{\tilde{\Phi}}^2 U_D^\dagger)_{33} \right] \\
&\quad + 6|\tilde{y}_t|^2 \left[ 2m_{\tilde{\Psi}_3}^2 + m_H^2 \right] + 4(|(\hat{\tilde{A}}_2)_{32}|^2 + |\tilde{A}_b|^2) + 6|\tilde{A}_t|^2, \\
\frac{d}{dt}m_{\tilde{N}_1}^2 &= 0, \\
\frac{d}{dt}m_{\tilde{N}_3}^2 &= 10|\tilde{y}_{\nu_3}|^2 \left[ m_{\tilde{N}_3}^2 + m_H^2 + m_{\tilde{\Phi}_3}^2 \right] + 10(|(\hat{\tilde{A}}_\nu)_{31}|^2 + |(\hat{\tilde{A}}_\nu)_{32}|^2 + |\tilde{A}_{\nu_3}|^2), \\
\frac{d}{dt}m_H^2 &= -\frac{96}{5}\kappa^2\tilde{\alpha}^3 + 6|\tilde{y}_t|^2 \left[ 2m_{\tilde{\Psi}_3}^2 + m_H^2 \right] + 2|\tilde{y}_{\nu_3}|^2 \left[ m_{\tilde{\Phi}_3}^2 + m_{\tilde{N}_3}^2 + m_H^2 \right] \\
&\quad + 2(|(\hat{\tilde{A}}_\nu)_{31}|^2 + |(\hat{\tilde{A}}_\nu)_{32}|^2 + |\tilde{A}_{\nu_3}|^2) + 6|\tilde{A}_t|^2, \\
\frac{d}{dt}m_{H'}^2 &= -\frac{96}{5}\kappa^2\tilde{\alpha}^3 + 8|\tilde{y}_b|^2 \left[ m_{\tilde{\Psi}_3}^2 + m_{H'}^2 + (U_D m_{\tilde{\Psi}}^2 U_D^\dagger)_{33} \right] \\
&\quad + 8(|(\hat{\tilde{A}}_2)_{32}|^2 + |\tilde{A}_b|^2).
\end{aligned} \tag{65}$$

## MSSM

In the last step, we evolve the soft masses down to  $M_Z$  using the RGE from [47].

$$\begin{aligned}
\frac{d}{dt}m_{\tilde{q}_1}^2 &= -\frac{32}{3}\kappa^2\tilde{\alpha}_3^3 - 6\kappa^2\tilde{\alpha}_2^3 - \frac{2}{15}\kappa^2\tilde{\alpha}_1^3 + \frac{1}{5}\frac{S_{\text{GUT}}}{\tilde{\alpha}_{\text{GUT}}}\tilde{\alpha}_1^2, \\
\frac{d}{dt}m_{\tilde{q}_3}^2 &= -\frac{32}{3}\kappa^2\tilde{\alpha}_3^3 - 6\kappa^2\tilde{\alpha}_2^3 - \frac{2}{15}\kappa^2\tilde{\alpha}_1^3 + \frac{1}{5}\frac{S_{\text{GUT}}}{\tilde{\alpha}_{\text{GUT}}}\tilde{\alpha}_1^2 \\
&\quad + 2|\tilde{y}_t|^2 \left[ m_{\tilde{q}_3}^2 + m_{H_u}^2 + m_{\tilde{u}_3}^2 \right] + 2|\tilde{y}_b|^2 \left[ m_{\tilde{q}_3}^2 + m_{H_d}^2 + (U_D m_d^2 U_D^\dagger)_{33} \right] \\
&\quad + 2(|\tilde{A}_t|^2 + |(\hat{\tilde{A}}_d)_{32}|^2 + |\tilde{A}_b|^2), \\
\frac{d}{dt}m_{\tilde{u}_1}^2 &= -\frac{32}{3}\kappa^2\tilde{\alpha}_3^3 - \frac{32}{15}\kappa^2\tilde{\alpha}_1^3 - \frac{4}{5}\frac{S_{\text{GUT}}}{\tilde{\alpha}_{\text{GUT}}}\tilde{\alpha}_1^2, \\
\frac{d}{dt}m_{\tilde{u}_3}^2 &= -\frac{32}{3}\kappa^2\tilde{\alpha}_3^3 - \frac{32}{15}\kappa^2\tilde{\alpha}_1^3 - \frac{4}{5}\frac{S_{\text{GUT}}}{\tilde{\alpha}_{\text{GUT}}}\tilde{\alpha}_1^2 \\
&\quad + 4|\tilde{y}_t|^2 \left[ m_{\tilde{u}_3}^2 + m_{\tilde{q}_3}^2 + m_{H_u}^2 \right] + 4|\tilde{A}_t|^2,
\end{aligned}$$

$$\begin{aligned}
\frac{d}{dt}m_{\tilde{d}_1}^2 &= -\frac{32}{3}\kappa^2\tilde{\alpha}_3^3 - \frac{8}{15}\kappa^2\tilde{\alpha}_1^3 + \frac{2}{5}\frac{S_{\text{GUT}}}{\tilde{\alpha}_{\text{GUT}}}\tilde{\alpha}_1^2 \\
&\quad + 4|\tilde{y}_b|^2|(U_D)_{31}|^2 \left[ m_{\tilde{d}_1}^2 + m_{\tilde{q}_3}^2 + m_{H_d}^2 \right] + 4(U_D^\dagger \hat{\tilde{A}}_d^\dagger \hat{\tilde{A}}_d U_D)_{11}, \\
\frac{d}{dt}m_{\tilde{d}_3}^2 &= -\frac{32}{3}\kappa^2\tilde{\alpha}_3^3 - \frac{8}{15}\kappa^2\tilde{\alpha}_1^3 + \frac{2}{5}\frac{S_{\text{GUT}}}{\tilde{\alpha}_{\text{GUT}}}\tilde{\alpha}_1^2 \\
&\quad + 4|\tilde{y}_b|^2|(U_D)_{33}|^2 \left[ m_{\tilde{d}_3}^2 + m_{\tilde{q}_3}^2 + m_{H_d}^2 \right] + 4(U_D^\dagger \hat{\tilde{A}}_d^\dagger \hat{\tilde{A}}_d U_D)_{33}, \\
\frac{d}{dt}m_{\tilde{l}_1}^2 &= -6\kappa^2\tilde{\alpha}_2^3 - \frac{6}{5}\kappa^2\tilde{\alpha}_1^3 - \frac{3}{5}\frac{S_{\text{GUT}}}{\tilde{\alpha}_{\text{GUT}}}\tilde{\alpha}_1^2 \\
&\quad + 2|\tilde{y}_\tau|^2|U_{31}|^2 \left[ m_{\tilde{l}_1}^2 + m_{H_d}^2 + m_{\tilde{l}_3}^2 \right] + 2(U^\dagger \hat{\tilde{A}}_e \hat{\tilde{A}}_e^\dagger U)_{11}, \\
\frac{d}{dt}m_{\tilde{l}_3}^2 &= -6\kappa^2\tilde{\alpha}_2^3 - \frac{6}{5}\kappa^2\tilde{\alpha}_1^3 - \frac{3}{5}\frac{S_{\text{GUT}}}{\tilde{\alpha}_{\text{GUT}}}\tilde{\alpha}_1^2 \\
&\quad + 2|\tilde{y}_\tau|^2|U_{33}|^2 \left[ 2m_{\tilde{l}_3}^2 + m_{H_d}^2 \right] + 2(U^\dagger \hat{\tilde{A}}_e \hat{\tilde{A}}_e^\dagger U)_{33}, \\
\frac{d}{dt}m_{\tilde{e}_1}^2 &= -\frac{24}{5}\kappa^2\tilde{\alpha}_1^3 + \frac{6}{5}\frac{S_{\text{GUT}}}{\tilde{\alpha}_{\text{GUT}}}\tilde{\alpha}_1^2, \\
\frac{d}{dt}m_{\tilde{e}_3}^2 &= -\frac{24}{5}\kappa^2\tilde{\alpha}_1^3 + \frac{6}{5}\frac{S_{\text{GUT}}}{\tilde{\alpha}_{\text{GUT}}}\tilde{\alpha}_1^2 \\
&\quad + 4|\tilde{y}_\tau|^2 \left[ m_{\tilde{e}_3}^2 + m_{H_d}^2 + (Um_{\tilde{l}}^2 U^\dagger)_{33} \right] + 4(|(\hat{\tilde{A}}_e)_{23}|^2 + |\tilde{A}_\tau|^2), \\
\frac{d}{dt}m_{H_u}^2 &= -6\kappa^2\tilde{\alpha}_2^3 - \frac{6}{5}\kappa^2\tilde{\alpha}_1^3 + \frac{3}{5}\frac{S_{\text{GUT}}}{\tilde{\alpha}_{\text{GUT}}}\tilde{\alpha}_1^2 \\
&\quad + 6|\tilde{y}_t|^2 \left[ m_{H_u}^2 + m_{\tilde{q}_3}^2 + m_{\tilde{u}_3}^2 \right] + 6|\tilde{A}_t|^2, \\
\frac{d}{dt}m_{H_d}^2 &= -6\kappa^2\tilde{\alpha}_2^3 - \frac{6}{5}\kappa^2\tilde{\alpha}_1^3 - \frac{3}{5}\frac{S_{\text{GUT}}}{\tilde{\alpha}_{\text{GUT}}}\tilde{\alpha}_1^2 \\
&\quad + 6|\tilde{y}_b|^2 \left[ m_{H_d}^2 + m_{\tilde{q}_3}^2 + (U_D m_{\tilde{d}}^2 U_D^\dagger)_{33} \right] + 2|\tilde{y}_\tau|^2 \left[ m_{H_d}^2 + m_{\tilde{l}_3}^2 + (Um_{\tilde{l}}^2 U^\dagger)_{33} \right] \\
&\quad + 6(|\tilde{A}_b|^2 + |(\hat{\tilde{A}}_d)_{32}|^2) + 2(|\tilde{A}_\tau|^2 + |(\hat{\tilde{A}}_e)_{23}|^2). \tag{66}
\end{aligned}$$

### 3.7 Parameters at $M_{\text{GUT}}$

The philosophy of the CMM model is somewhat different from that of the CMSSM. Although both need only a few input parameters and are in a sense minimal flavor violating, the CMSSM assumes flavor universality at the GUT scale with quark and lepton flavor structures being unrelated. By contrast, the CMM model invokes universality (see Eq. (18)) at a more natural scale, namely  $M_{\text{Pl}}$ . All flavor violation stems from a non-renormalizable term related to  $Y_d$  due to the assumption that the Majorana mass matrix and the up Yukawa coupling are simultaneously diagonalizable. Furthermore, the CMM model is minimal in the sense that it is only constructed with Higgs representations that are needed for symmetry breaking anyway.

Contrary to the CMSSM, at the GUT scale universality is already broken in the CMM model due to the running  $M_{\text{Pl}} \rightarrow M_{\text{SO}(10)} \rightarrow M_{\text{GUT}}$ . We illustrate the difference with the input parameters  $M_{\tilde{q}} = 1500$  GeV,  $m_{\tilde{g}_3} = 500$  GeV,  $a_1^d(M_Z)/M_{\tilde{q}} = 1.5$ ,  $\arg(\mu) = 0$  and  $\tan\beta = 6$ . With our running

procedure the universal parameters at the Planck scale have the values:

$$a_0 = 1273 \text{ GeV}, \quad m_0 = 1430 \text{ GeV}, \quad m_{\tilde{g}} = 184 \text{ GeV}. \quad (67)$$

Using the super-CKM basis (as denoted by the hat) for the trilinear terms and the up basis for masses, we already arrive at the following non-universal parameters at the GUT scale:

$$\hat{\mathbf{A}}_u(M_{\text{GUT}}) = \begin{pmatrix} 0 & 0 & 0 \\ 0 & 0 & 0 \\ 0 & 0 & 46 \end{pmatrix} \text{ GeV}, \quad \hat{\mathbf{A}}_d(M_{\text{GUT}}) = \begin{pmatrix} 0 & 0 & 0 \\ 0 & 0 & 0 \\ 0 & 0.3 & -3.5 \end{pmatrix} \text{ GeV}, \quad (68a)$$

$$\hat{\mathbf{A}}_\nu(M_{\text{GUT}}) = \begin{pmatrix} 0 & 0 & 0 \\ 0 & 0 & 0 \\ -0.0013 & 0.0023 & 43.4 \end{pmatrix} \text{ GeV}, \quad (68b)$$

$$m_{\tilde{\Phi}}(M_{\text{GUT}}) = \text{diag}(1426, 1426, 1074) \text{ GeV}, \quad (68c)$$

$$m_{\tilde{\Psi}}(M_{\text{GUT}}) = \text{diag}(1444, 1444, 1077) \text{ GeV}, \quad (68d)$$

$$m_{\tilde{N}}(M_{\text{GUT}}) = \text{diag}(1459, 1459, 1078) \text{ GeV}, \quad (68e)$$

$$m_{H_u}(M_{\text{GUT}}) = 1126 \text{ GeV}, \quad m_{H_d}(M_{\text{GUT}}) = 1446 \text{ GeV}, \quad (68f)$$

$$m_{\tilde{g}}(M_{\text{GUT}}) = 211 \text{ GeV}. \quad (68g)$$

With  $\tilde{y}_t(M_{\text{GUT}}) = 0.046$  and  $\tilde{y}_b(M_{\text{GUT}}) = -0.0026$  we can now no longer write  $\mathbf{A} = a_0 \mathbf{Y}$ , especially  $\mathbf{A}_d$  has already developed an off-diagonal entry inducing  $\tilde{s}_R \rightarrow \tilde{b}_L$ -transitions. Moreover, the third generation masses already separate significantly from those of the first two generations at the GUT scale.

The idea of universal soft breaking terms at  $M_{\text{Pl}}$  and flavor-violation from  $y_t$ -driven RG running above  $M_{\text{GUT}}$  has been studied by many authors, both in  $\text{SU}(5)$  and  $\text{SO}(10)$  scenarios [10, 12–14, 18, 22, 51–54]. A detailed comparison of our results with the literature will be given in Sec. 6.

## 4 Observables

In this Section, we briefly summarize the observables that are used to constrain the CMM model parameter space.

### 4.1 $B_s - \bar{B}_s$ Mixing

$B_s - \bar{B}_s$  oscillations are governed by the Schrödinger equation

$$i \frac{d}{dt} \begin{pmatrix} |B_s(t)\rangle \\ |\bar{B}_s(t)\rangle \end{pmatrix} = \left( \mathbf{M}^s - \frac{i}{2} \Gamma^s \right) \begin{pmatrix} |B_s(t)\rangle \\ |\bar{B}_s(t)\rangle \end{pmatrix} \quad (69)$$

with the mass matrix  $\mathbf{M}^s$  and the decay matrix  $\Gamma^s$ . The physical eigenstates  $|B_{H,L}\rangle$  with the masses  $M_{H,L}$  and the decay rates  $\Gamma_{H,L}$  are obtained by diagonalizing  $\mathbf{M}^s - i\Gamma^s/2$ . The physical observables

are the mass and width differences as well as the CP phase,

$$\begin{aligned}\Delta M_s &= M_H^s - M_L^s = 2 |\mathbf{M}_{12}^s|, \\ \Delta \Gamma_s &= \Gamma_L^s - \Gamma_H^s = 2 |\Gamma_{12}^s| \cos \phi_s, \\ \phi_s &= \arg \left( -\frac{\mathbf{M}_{12}^s}{\Gamma_{12}^s} \right).\end{aligned}\tag{70}$$

In the CMM model, there are two operators contributing to the oscillations,

$$\mathcal{O}_L = \bar{s}_{L,\alpha} \gamma_\mu b_{L,\alpha} \bar{s}_{L,\beta} \gamma^\mu b_{L,\beta} \tag{71a}$$

$$\mathcal{O}_R = \bar{s}_{R,\alpha} \gamma_\mu b_{R,\alpha} \bar{s}_{R,\beta} \gamma^\mu b_{R,\beta} . \tag{71b}$$

In the standard model, only the left-handed operator (71a) is present due to the absence of the right-handed vector bosons. With weak-scale supersymmetry, however, the vertices in Fig. 1 contribute to both  $\mathcal{O}_L$  and  $\mathcal{O}_R$  with the quark-squark-gluino vertex in Fig. 1(a) dominating.

The  $B_s - \bar{B}_s$  oscillations are governed by

$$\mathbf{M}_{12,\text{CMM}}^s = \frac{G_F^2 M_W^2 M_{B_s}}{12\pi^2} \left( f_{B_s}^2 \hat{B}_{B_s} \right) (V_{ts}^* V_{tb})^2 (C_L(\mu_b) + C_R(\mu_b)) . \tag{72}$$

Here  $G_F$  is the Fermi constant,  $M_{B_s}$  and  $M_W$  are the masses of  $B_s$  meson and  $W$ -boson, respectively. The renormalization scale entering the Wilson coefficients  $C_{L,R}$  is  $\mu_b \sim m_b$ . The long-distance QCD effects are contained in the equal hadronic matrix element of  $\mathcal{O}_{L,R}$  and are parametrized by

$$f_{B_s} \sqrt{\hat{B}_{B_s}} = (0.2580 \pm 0.0195) \text{ GeV} , \tag{73}$$

where we use the values listed in [55]:  $f_{B_s} = 228 \pm 3 \pm 17 \text{ MeV}$  and  $\hat{B}_{B_s} = 1.28 \pm 0.02 \pm 0.03$ . Finally, the coefficients  $C_L$  and  $C_R$  read<sup>7</sup>

$$C_L(\mu_b) = \eta_B F_{tt} , \tag{74}$$

$$C_R(\mu_b) = \frac{(U_D^{23*} U_D^{33})^2}{(V_{ts}^* V_{tb})^2} \frac{8\pi^2 \alpha_s^2(M_Z)}{G_F^2 M_W^2 m_{g_3}^2} \eta_B S^{(\tilde{g})}(x, y), \tag{75}$$

where  $\eta_B = 0.55$  [56], the function  $F_{tt}$  is given e.g. in Eq. (4.5) of [57] and  $S^{(\tilde{g})}(x, y)$  denotes the loop function

$$\begin{aligned}S^{(\tilde{g})}(x, y) &= \frac{11}{18} [G(x, x) + G(y, y) - 2G(x, y)] - \frac{2}{9} [F(x, x) + F(y, y) - 2F(x, y)] , \\ F(x, y) &= \frac{1}{y-x} \left[ \frac{x \ln x}{(x-1)^2} - \frac{1}{x-1} - (x \leftrightarrow y) \right] , \\ G(x, y) &= \frac{1}{x-y} \left[ \frac{x^2 \ln x}{(x-1)^2} - \frac{1}{x-1} - (x \leftrightarrow y) \right] , \quad x = \frac{m_{d_2}^2}{m_{g_3}^2}, \quad y = \frac{m_{d_3}^2}{m_{g_3}^2} .\end{aligned}\tag{76}$$

---

<sup>7</sup>Note, that in [38]  $C_{L,R}$  include the factor  $r = 0.985$  which removes the NLO QCD corrections to  $S_0(x_t)$  in the SM.

Next we insert  $U_D^{i3}$  from Eq. (15) into Eq. (75) to make the dependence on the new CP phase  $\xi$  explicit:

$$C = C_L + e^{-2i\xi} |C_R^{\text{CMM}}|, \quad (77)$$

In Eqs. (75) and (77) we have, in the spirit of this paper, concentrated on the dominant new effect involving large parameters (namely  $\xi$  and the atmospheric neutrino mixing angle). Among the neglected effects are the MFV-like contributions proportional to  $V_{ts}^{*2}$  involving left-handed squarks and gluinos. These contributions are not only small in magnitude compared to the second term in Eq. (77) (a few percent of the SM coefficient), they are also in phase with the SM contribution and do not alter the CP asymmetries in  $B_s - \bar{B}_s$  mixing. The MFV boxes involving charged Higgs bosons and those with charginos and squarks could be neglected as well, but are nevertheless included in our analysis through the function  $F_{tt}$  of [57]. The free phase  $\xi$  is essential: First, it is the source of a possibly large CP phase  $\arg C$  and second, it may tame the CMM contribution to  $\Delta M_s$ , which for  $\xi = 0$  can easily exceed the experimental bound. But with a non-zero  $\xi$  the two contributions in Eq. (77) can be arranged to keep  $|C|$  in the range complying within the allowed region for  $\Delta M_s$ . Since  $\xi$  and  $\xi + \pi$  cannot be distinguished in  $B_s - \bar{B}_s$  mixing, we only consider the case  $\xi \in [0, \pi]$ , noting that  $b \rightarrow s\gamma$  depends only weakly on this phase. Mixing-induced CP asymmetries in  $b \rightarrow s$  penguin decays constitute a possibility to distinguish between  $\xi$  and  $\xi + \pi$ , with  $a_{\text{CP}}^{\text{mix}}(B_d \rightarrow \phi K_S) < a_{\text{CP}}^{\text{mix,SM}}(B_d \rightarrow \phi K_S)$  favoring  $\xi \in [0, \pi]$ .

The current experimental status is as follows. The CDF experiment measured the mass difference to be [24],

$$\Delta M_s = (17.77 \pm 0.10 \text{ (stat.)} \pm 0.07 \text{ (syst.)}) \text{ ps}^{-1}, \quad (78)$$

in agreement with the DØ range and the SM prediction [58],

$$\Delta M_s^{\text{SM}} = (19.30 \pm 6.68) \text{ ps}^{-1}. \quad (79)$$

Combining both experiments gives [50]

$$\Delta M_s^{\text{PDG}} = (17.77 \pm 0.12) \text{ ps}^{-1}. \quad (80)$$

The SM CP phase in Eq. (70) is small [55, 58],

$$\phi_s^{\text{SM}} = (4.3_{-3.1}^{+3.5}) \times 10^{-3}. \quad (81)$$

The CP phase has been constrained by both the CDF and DØ collaborations in different ways. The angular analysis of tagged  $B_s \rightarrow J/\psi\phi$  decays determines  $2\beta_s$ , with SM value  $\beta_s^{\text{SM}} = -\arg\left(-\frac{V_{ts}^* V_{tb}}{V_{cs}^* V_{cb}}\right) = 0.01811_{-0.00082}^{+0.0085}$  [55]. Neglecting the tiny  $\phi_s^{\text{SM}}$ , new physics in  $M_{12}^s$  will lead to  $2\beta_s = 2\beta_s^{\text{SM}} - \phi_s$  and  $\phi_s$  in Eq. (70) can a-priori be of order 1. The new results for  $2\beta_s$  presented in summer 2010 are given as [27, 28]

$$-2\beta_s^{\text{CDF}} \equiv -2\beta_s^{\text{SM}} + \phi_s \in [-1.04, -0.04] \cup [-3.10, -2.16] \quad (68\% \text{ CL}), \quad (82a)$$

$$\in [-\pi, -1.78] \cup [-1.36, 0.26] \cup [2.88, \pi] \quad (95\% \text{ CL}) \quad (82b)$$

$$\phi_s^{\text{DØ}} \equiv -2\beta_s^{\text{SM}} + \phi_s = -0.76_{-0.36}^{+0.38} \text{ (stat)} \pm 0.02 \text{ (syst)} \quad (82c)$$

$$\in [-1.65, 0.24] \cup [1.14, 2.93] \quad (95\% \text{ CL}). \quad (82d)$$



So far there is no combination of the CDF and DØ results available. Recently DØ has measured the inclusive dimuon asymmetry  $A^b = \frac{N_b^{++} - N_b^{--}}{N_b^{++} + N_b^{--}}$  using  $6.1 \text{ fb}^{-1}$  of integrated luminosity where  $N_b^{++}$  counts the number of  $(B^0(t), \bar{B}^0(t)) \rightarrow (\mu^+, \mu^+)$  and  $N_b^{--}$  decays into  $(\mu^-, \mu^-)$  [29]. The same asymmetry can also be obtained from semileptonic decays  $a_{\text{fs}} = \frac{\Gamma(\bar{B}^0 \rightarrow X \ell^+ \nu_\ell) - \Gamma(B^0 \rightarrow \bar{X} \ell^- \bar{\nu}_\ell)}{\Gamma(\bar{B}^0 \rightarrow X \ell^+ \nu_\ell) + \Gamma(B^0 \rightarrow \bar{X} \ell^- \bar{\nu}_\ell)} = A^b$ . The two measurements combine to [29]

$$a_{\text{fs}} = -0.00957 \pm 0.00251 \pm 0.00146 \quad (83)$$

for a mixture between  $B_d$ - and  $B_s$ -mesons with

$$a_{\text{fs}} = (0.506 \pm 0.043) a_{fs}^d + (0.494 \pm 0.043) a_{fs}^s. \quad (84)$$

Comparison with the predicted SM value  $a_{\text{fs}}^{\text{SM}} = (-0.23_{-0.06}^{+0.05}) \cdot 10^{-3}$  [58] yields a  $3.2\sigma$  discrepancy. Averaging with the CDF result  $a_{\text{fs}} = 0.008 \pm 0.0090 \pm 0.0068$  [30] results in a  $2.9\sigma$  deviation from the SM:

$$a_{\text{fs}} = -0.0085 \pm 0.0028 \quad \text{at 68\% CL.} \quad (85)$$

The relation with the CP phase  $\phi_s$  is given by  $a_{\text{fs}}^s = \frac{|\Gamma_{12}^s|}{|\mathbf{M}_{12}^s|} \sin \phi_s$ . Assuming there is no new physics in  $a_{\text{fs}}^d$  the experimental value translates into  $a_{\text{fs}}^s = -0.017 \pm 0.056$  which corresponds to

$$\sin \phi_s = -2.2 \pm 1.4 \quad \text{at 95\% CL,} \quad (86)$$

with a central value in the unphysical region. For our numerical analysis we naively use a weighted average of the experimental values for  $\sin \phi_s$  only employing the second interval in (82b) and the first in (82d), as well as eq. (86). At 95% CL we obtain

$$\sin \phi_s = -0.77 \pm 0.47. \quad (87)$$

The global analysis in [55] found also hints of new physics in  $B_d - \bar{B}_d$  mixing, which alleviates the problem in Eq. (86). The best-fit value for the corresponding CP phase  $\phi_d$  is much smaller in magnitude than  $\phi_s$ . In [38] it has been shown that a non-zero  $\phi_d$  and a phenomenologically equally welcome contribution to  $\epsilon_K$  can arise in the CMM model from dimension-5 Yukawa terms. In this paper we do not consider these sub-dominant terms which would introduce new parameters to the analysis.

## 4.2 $b \rightarrow s\gamma$

The atmospheric mixing angle in  $U_D$  has a strong impact in  $b \rightarrow s\gamma$ . In the SM it is mediated via a  $W$  boson in which the  $b_L \rightarrow s_R$ -transition is proportional to the strange quark mass  $\propto m_s$  and thus negligible compared to the  $b_R \rightarrow s_L$ -transition  $\propto m_b$ . In the CMM model amplitudes with both chiralities occur:

$$\mathcal{A}(b_L \rightarrow s_R \gamma) \propto \left( U_D m_d^2 U_D^\dagger \right)_{32} \rightarrow C'_7 \quad (88)$$

$$\mathcal{A}(b_R \rightarrow s_L \gamma) \propto \left( V_q^\dagger m_q^2 V_q \right)_{32} \rightarrow C_7. \quad (89)$$

Eq. (88) is the effect of the genuine  $\tilde{b}_R\text{--}\tilde{s}_L$  transition of the CMM model. It contributes to  $C'_7$  and therefore yields a positive contribution to  $\mathcal{B}(b \rightarrow s\gamma)$ . The term in Eq. (89) constitutes an MFV-like (i.e. CKM-driven) gluino-squark contribution to  $C_7$ . We will see later that in the ballpark of the viable parameter region of the model the second contribution is larger and actually reduces  $\mathcal{B}(b \rightarrow s\gamma)$ . This is the only place where we find a formally subdominant (namely CKM-suppressed) contribution important. Its relevance stems partially from the interference of the term in Eq. (89) with the SM term. Therefore the contribution in Eq. (89) enters  $\mathcal{B}(b \rightarrow s\gamma)$  linearly, while the one in Eq. (88) modifies this branching ratio quadratically.

The branching ratio for  $b \rightarrow s\gamma$  is usually written as

$$\mathcal{B}(b \rightarrow s\gamma) = \mathcal{B}_{SL} \frac{6 |V_{tb} V_{ts}^*|^2}{\pi |V_{cb}|^2 g (m_c^2/m_b^2)} \left( |\hat{C}_7(\mu_b)|^2 + |\hat{C}'_7(\mu_b)|^2 \right), \quad (90)$$

where  $\mathcal{B}_{SL} = 0.1033 \pm 0.0028$  [50] is semileptonic branching ratio and  $g(z) = 1 - 8z + 8z^3 - z^4 - 12z^2 \ln(z)$ . The effective Wilson coefficients are given by [59, 60]

$$\begin{aligned} \hat{C}_7(\mu_b) &= C_7^{\text{eff}}(\mu_b) - \left[ C_{7b\tilde{g}}(\mu_b) + \frac{1}{m_b} C_{7\tilde{g}\tilde{g}}(\mu_b) \right] \frac{16\sqrt{2}\pi^3\alpha_s(\mu_b)}{G_F V_{tb} V_{ts}^*}, \\ \hat{C}'_7(\mu_b) &= C'_7(\mu_b) - \left[ C'_{7b\tilde{g}}(\mu_b) + \frac{1}{m_b} C'_{7\tilde{g}\tilde{g}}(\mu_b) \right] \frac{16\sqrt{2}\pi^3\alpha_s(\mu_b)}{G_F V_{tb} V_{ts}^*}, \end{aligned} \quad (91)$$

where  $\alpha_s$  is the strong gauge coupling. The RGE evolution to the scale  $\mu_b$  is given by

$$C_{7b\tilde{g}}(\mu_b) = \eta^{\frac{39}{23}} C_{7b\tilde{g}}(\mu_W) + \frac{8}{3} \left( \eta^{\frac{37}{23}} - \eta^{\frac{39}{23}} \right) C_{8b\tilde{g}}(\mu_W), \quad (92)$$

$$C_{7\tilde{g}\tilde{g}}(\mu_b) = \eta^{\frac{27}{23}} C_{7\tilde{g}\tilde{g}}(\mu_W) + \frac{8}{3} \left( \eta^{\frac{25}{23}} - \eta^{\frac{27}{23}} \right) C_{8\tilde{g}\tilde{g}}(\mu_W) \quad (93)$$

(for the running of the primed coefficients, substitute  $C'_i$  for  $C_i$ );

$$C_7^{\text{eff}}(\mu_b) = C_7^{\text{SM}}(\mu_b) + \eta^{\frac{16}{23}} C_7(\mu_W) + \frac{8}{3} \left( \eta^{\frac{14}{23}} - \eta^{\frac{16}{23}} \right) C_8(\mu_W), \quad (94)$$

$$C'_7(\mu_b) = \eta^{\frac{16}{23}} C'_7(\mu_W) + \frac{8}{3} \left( \eta^{\frac{14}{23}} - \eta^{\frac{16}{23}} \right) C'_8(\mu_W) \quad (95)$$

and

$$\eta \equiv \frac{\alpha_s(\mu_W)}{\alpha_s(\mu_b)}. \quad (96)$$

For the SM contribution we use

$$C_7^{\text{SM}}(\mu_b) = -0.335. \quad (97)$$

Without new physics contribution this value reproduces the SM NNLO result [61]:

$$\mathcal{B}(b \rightarrow s\gamma)_{E_\gamma > 1.6 \text{ GeV}}^{\text{SM}} = (3.15 \pm 0.23) \times 10^{-4}. \quad (98)$$

An average of the experimental data of BABAR, Belle and CLEO yields [62]:

$$\mathcal{B}(b \rightarrow s\gamma)_{E_\gamma > 1.6 \text{ GeV}}^{\text{exp}} = (3.55 \pm 0.24_{-0.10}^{+0.09} \pm 0.03) \times 10^{-4}, \quad (99)$$

where the errors are combined statistical and systematic, systematic due to the shape function, and the  $b \rightarrow d\gamma$  fraction. The SM prediction lies within the  $3\sigma$  range, but since the central values differ from each other there is still room for new physics.

The MSSM contributions are computed with the following formulas [59,60] (using the abbreviation  $V \doteq (4G_F V_{tb}V_{ts}^*)/\sqrt{2}$ ): The chargino-, neutralino- and Higgs contributions read:

$$\begin{aligned}
C_7(\mu_W) = & -\frac{1}{2} [\cot^2 \beta x_{tH}(Q_u F_1(x_{tH}) + F_2(x_{tH})) + x_{tH}(Q_u F_3(x_{tH}) + F_4(x_{tH}))] \\
& + \frac{1}{2V} \sum_{j=1}^6 \sum_{l=1}^2 \frac{1}{m_{\tilde{u}_j}^2} B_{2j\ell}^d B_{3j\ell}^{d*} [F_1(x_{\tilde{\chi}_\ell^\pm \tilde{u}_j}) + Q_u F_2(x_{\tilde{\chi}_\ell^\pm \tilde{u}_j})] \\
& + \frac{1}{2V} \sum_{j=1}^6 \sum_{l=1}^2 \frac{1}{m_{\tilde{u}_j}^2} \frac{m_{\tilde{\chi}_\ell^\pm}}{m_b} B_{2j\ell}^d A_{3j\ell}^{d*} [F_3(x_{\tilde{\chi}_\ell^\pm \tilde{u}_j}) + Q_u F_4(x_{\tilde{\chi}_\ell^\pm \tilde{u}_j})] \\
& + \frac{Q_d}{2V} \sum_{j=1}^6 \sum_{l=1}^4 \frac{1}{m_{\tilde{d}_j}^2} \left[ D_{2j\ell}^d D_{3j\ell}^{d*} F_2(x_{\tilde{\chi}_\ell^0 \tilde{d}_j}) + \frac{m_{\tilde{\chi}_\ell^0}}{m_b} D_{2j\ell}^d C_{3j\ell}^{d*} F_4(x_{\tilde{\chi}_\ell^0 \tilde{d}_j}) \right] \quad (100)
\end{aligned}$$

$$\begin{aligned}
C_8(\mu_W) = & -\frac{1}{2} [\cot^2 \beta x_{tH} F_1(x_{tH}) + x_{tH} F_3(x_{tH})] \\
& + \frac{1}{2V} \sum_{j=1}^6 \sum_{l=1}^2 \frac{1}{m_{\tilde{u}_j}^2} \left[ B_{2j\ell}^d B_{3j\ell}^{d*} F_2(x_{\tilde{\chi}_\ell^\pm \tilde{u}_j}) + \frac{m_{\tilde{\chi}_\ell^\pm}}{m_b} B_{2j\ell}^d A_{3j\ell}^{d*} F_4(x_{\tilde{\chi}_\ell^\pm \tilde{u}_j}) \right] \\
& + \frac{1}{2V} \sum_{j=1}^6 \sum_{l=1}^4 \frac{1}{m_{\tilde{d}_j}^2} \left[ D_{2j\ell}^d D_{3j\ell}^{d*} F_2(x_{\tilde{\chi}_\ell^0 \tilde{d}_j}) + \frac{m_{\tilde{\chi}_\ell^0}}{m_b} D_{2j\ell}^d C_{3j\ell}^{d*} F_4(x_{\tilde{\chi}_\ell^0 \tilde{d}_j}) \right] \quad (101)
\end{aligned}$$

$$\begin{aligned}
C'_7(\mu_W) = & -\frac{1}{2} \frac{m_s m_b}{m_t^2} \tan^2 \beta x_{tH} (Q_u F_1(x_{tH}) + F_2(x_{tH})) \\
& + \frac{1}{2V} \sum_{j=1}^6 \sum_{l=1}^2 \frac{1}{m_{\tilde{u}_j}^2} A_{2j\ell}^d A_{3j\ell}^{d*} [F_1(x_{\tilde{\chi}_\ell^\pm \tilde{u}_j}) + Q_u F_2(x_{\tilde{\chi}_\ell^\pm \tilde{u}_j})] \\
& + \frac{1}{2V} \sum_{j=1}^6 \sum_{l=1}^2 \frac{1}{m_{\tilde{u}_j}^2} \frac{m_{\tilde{\chi}_\ell^\pm}}{m_b} A_{2j\ell}^d B_{3j\ell}^{d*} [F_3(x_{\tilde{\chi}_\ell^\pm \tilde{u}_j}) + Q_u F_4(x_{\tilde{\chi}_\ell^\pm \tilde{u}_j})] \\
& + \frac{Q_d}{2V} \sum_{j=1}^6 \sum_{l=1}^4 \frac{1}{m_{\tilde{d}_j}^2} \left[ C_{2j\ell}^d C_{3j\ell}^{d*} F_2(x_{\tilde{\chi}_\ell^0 \tilde{d}_j}) + \frac{m_{\tilde{\chi}_\ell^0}}{m_b} C_{2j\ell}^d D_{3j\ell}^{d*} F_4(x_{\tilde{\chi}_\ell^0 \tilde{d}_j}) \right] \quad (102)
\end{aligned}$$

$$\begin{aligned}
C'_8(\mu_W) = & -\frac{1}{2} \frac{m_s m_b}{m_t^2} \tan^2 \beta x_{tH} F_1(x_{tH}) \\
& + \frac{1}{2V} \sum_{j=1}^6 \sum_{l=1}^2 \frac{1}{m_{\tilde{u}_j}^2} \left[ A_{2j\ell}^d A_{3j\ell}^{d*} F_2(x_{\tilde{\chi}_\ell^\pm \tilde{u}_j}) + \frac{m_{\tilde{\chi}_\ell^\pm}}{m_b} A_{2j\ell}^d B_{3j\ell}^{d*} F_4(x_{\tilde{\chi}_\ell^\pm \tilde{u}_j}) \right] \\
& + \frac{1}{2V} \sum_{j=1}^6 \sum_{l=1}^4 \frac{1}{m_{\tilde{d}_j}^2} \left[ C_{2j\ell}^d C_{3j\ell}^{d*} F_2(x_{\tilde{\chi}_\ell^0 \tilde{d}_j}) + \frac{m_{\tilde{\chi}_\ell^0}}{m_b} C_{2j\ell}^d D_{3j\ell}^{d*} F_4(x_{\tilde{\chi}_\ell^0 \tilde{d}_j}) \right], \quad (103)
\end{aligned}$$

where  $Q_u = 2/3$ ,  $Q_d = -1/3$ ,  $x_{\tilde{\chi}_\ell^{0,\pm} \tilde{q}_j} = m_{\tilde{\chi}_\ell^{0,\pm}}^2/m_{\tilde{q}_j}^2$  and  $x_{tH} = m_t^2/m_{H^\pm}^2$ . The gluino contributions

read:

$$\begin{aligned}
C_{7b,\tilde{g}}(\mu_W) &= -\frac{Q_d}{16\pi^2} \frac{4}{3} \sum_{k=1}^6 \frac{1}{m_{\tilde{d}_k}^2} \left( \Gamma_{DL}^{kb} \Gamma_{DL}^{*ks} \right) F_2(x_{gd_k}) , \\
C_{7\tilde{g},\tilde{g}}(\mu_W) &= m_{\tilde{g}_3} \frac{Q_d}{16\pi^2} \frac{4}{3} \sum_{k=1}^6 \frac{1}{m_{\tilde{d}_k}^2} \left( \Gamma_{DR}^{kb} \Gamma_{DL}^{*ks} \right) F_4(x_{gd_k}) , \\
C_{8b,\tilde{g}}(\mu_W) &= -\frac{1}{16\pi^2} \sum_{k=1}^6 \frac{1}{m_{\tilde{d}_k}^2} \left( \Gamma_{DL}^{kb} \Gamma_{DL}^{*ks} \right) \left[ -\frac{1}{6} F_2(x_{gd_k}) - \frac{3}{2} F_1(x_{gd_k}) \right] , \\
C_{8\tilde{g},\tilde{g}}(\mu_W) &= m_{\tilde{g}_3} \frac{1}{16\pi^2} \sum_{k=1}^6 \frac{1}{m_{\tilde{d}_k}^2} \left( \Gamma_{DR}^{kb} \Gamma_{DL}^{*ks} \right) \left[ -\frac{1}{6} F_4(x_{gd_k}) - \frac{3}{2} F_3(x_{gd_k}) \right] . \tag{104}
\end{aligned}$$

The ratios  $x_{gd_k}$  are defined as  $x_{gd_k} \equiv m_{\tilde{g}}^2/m_{\tilde{d}_k}^2$ . The Wilson coefficients of the corresponding primed operators are obtained through the interchange  $\Gamma_{DR}^{ij} \leftrightarrow \Gamma_{DL}^{ij}$ . Finally, we define the functions  $F_i$  appearing in the Wilson coefficients listed above:

$$\begin{aligned}
F_1(x) &= \frac{1}{12(x-1)^4} (x^3 - 6x^2 + 3x + 2 + 6x \log x) , \\
F_2(x) &= \frac{1}{12(x-1)^4} (2x^3 + 3x^2 - 6x + 1 - 6x^2 \log x) , \\
F_3(x) &= \frac{1}{2(x-1)^3} (x^2 - 4x + 3 + 2 \log x) , \\
F_4(x) &= \frac{1}{2(x-1)^3} (x^2 - 1 - 2x \log x) . \tag{105}
\end{aligned}$$

The matrices appearing in the above expressions are now expressed in terms of the mixing matrices according to the convention of [40] except for the vacuum expectation values:

$$v_1^{[59]} = \frac{1}{\sqrt{2}} v_1^{[40]} , \quad v_2^{[59]} = \frac{1}{\sqrt{2}} v_2^{[40]} \tag{106}$$

The mixing matrices of up and down quarks are

$$(\Gamma_{DL})_{iI} = Z_D^{Ii} \quad (\Gamma_{DR})_{iI} = Z_D^{(I+3)i} \tag{107}$$

$$(\Gamma_{UL})_{iI} = Z_U^{Ii*} \quad (\Gamma_{UR})_{iI} = Z_U^{(I+3)i*} . \tag{108}$$

Other abbreviations that appear are:

$$A_{ijl}^d = \frac{e}{\sqrt{2} \sin \theta_W M_W \cos \beta} M_d^{ik} Z_U^{kj} Z_-^{2l} \tag{109}$$

$$B_{ijl}^d = \frac{e}{\sqrt{2} \sin \theta_W M_W \sin \beta} \left( K^\dagger M_u \right)^{ik} Z_U^{(k+3)j} Z_+^{2l*} - \frac{e}{\sin \theta_W} Z_U^{ij} Z_+^{1l*} \tag{110}$$

$$C_{ijl}^d = \frac{e}{\sqrt{2} \sin \theta_W M_W \cos \beta} M_d^{ik} Z_D^{kj*} Z_N^{3l} - \frac{\sqrt{2}e}{\cos \theta_W} Q_d Z_D^{(i+3)j*} Z_N^{1l} \tag{111}$$

$$D_{ijl}^d = \frac{e}{\sqrt{2} \sin \theta_W M_W \cos \beta} M_d^{ik} Z_D^{(k+3)j*} Z_N^{3l*} + \frac{1}{\sqrt{2}} Z_D^{ij*} \left[ (2Q_d + 1) \frac{e}{\cos \theta_W} Z_N^{1l*} - \frac{e}{\sin \theta_W} Z_N^{2l*} \right] \tag{112}$$

where  $M_u$  and  $M_d$  are diagonal  $3 \times 3$ -matrices that contain the masses of up and down quarks respectively in their diagonal elements. All mixing matrices are according to [40]. For completeness we also list the conversion of conventions for the mixing matrices of charginos, neutralinos and charged Higgs bosons:

$$U = Z_-^\dagger, \quad V = Z_+^\dagger, \quad N = Z_N^\dagger, \quad Z_E = Z_H^\dagger. \quad (113)$$

### 4.3 $\tau \rightarrow \mu\gamma$

So far, large transitions in the observables we have looked at stem from a large mixing among the right-handed down-type squarks, induced by GUT relations. Therefore, it is important to correlate those results with the results from a decay in the lepton sector where the PMNS matrix is directly responsible for the transition:  $\tau \rightarrow \mu\gamma$ . In the SM with massive neutrinos this decay is unobservably small, such that any signal would be a clear proof for new physics. The experimental upper bounds are:

$$\mathcal{B}(\tau \rightarrow \mu\gamma)^{\text{exp}} < 4.5 \times 10^{-8} \quad \text{at 90\% CL (Belle) [63]} \quad (114)$$

$$\mathcal{B}(\tau \rightarrow \mu\gamma)^{\text{exp}} < 4.4 \times 10^{-8} \quad \text{at 90\% CL (BaBar) [64]}. \quad (115)$$

In the CMM model the atmospheric mixing angle enters  $Z_L$  and the PMNS matrix itself in slepton-neutralino and chargino-sneutrino vertices. We use the one-loop result of [65] but employ the notation of [66] and correction of a factor  $\cos\theta_W$ . Furthermore, we consider a limit which is suitable for the CMM model: Setting  $y_\mu = 0$ , we consider only  $\tau_R \rightarrow \mu_L\gamma$  transitions. The branching ratio reads:

$$\mathcal{B}(\tau \rightarrow \mu\gamma) = \frac{\tau_\tau m_\tau^5}{4\pi} \left| C_7^{\tilde{\chi}^\pm} + C_7^{\tilde{\chi}^0} \right|^2 \quad (116)$$

with the  $\tau$  lifetime  $\tau_\tau = 290.6 \times 10^{-15}$  s and the  $\tau$  mass  $m_\tau = 1.77699$  GeV [50]. The Wilson coefficients are given by:

$$C_7^{\tilde{\chi}^\pm} = \frac{e^3}{32\pi^2 \sin^2 \theta_W} \sum_{J=1}^3 \sum_{i=1}^2 U_D^{2J} U_D^{3J*} \left[ Z_+^{1i*} Z_+^{1i} \frac{H_1(x_{Ji})}{m_{\chi_i^+}^2} - Z_+^{1i*} Z_-^{2i*} \frac{H_2(x_{Ji})}{\sqrt{2} \cos \beta m_{\chi_i^+} M_W} \right] \quad (117)$$

$$\begin{aligned} C_7^{\tilde{\chi}^0} = & \frac{e^3}{32\pi^2 \sin^2 \theta_W} \sum_{J=1}^6 \sum_{i=1}^4 \frac{1}{m_{\chi_i^0}^2} \left[ Z_L^{2J*} Z_L^{3J} |Z_N^{1i} \sin \theta_W + Z_N^{2i} \cos \theta_W|^2 \frac{H_3(y_{Ji})}{2 \cos^2 \theta_W} \right. \\ & - Z_L^{2J*} Z_L^{6J} Z_N^{3i} (Z_N^{1i*} \sin \theta_W + Z_N^{2i*} \cos \theta_W) \frac{m_\tau H_3(y_{Ji})}{2 \cos \theta_W M_W \cos \beta} \\ & + Z_L^{2J*} Z_L^{3J} Z_N^{3i*} (Z_N^{1i*} \sin \theta_W + Z_N^{2i*} \cos \theta_W) \frac{m_{\chi_i^0} H_4(y_{Ji})}{2 \cos \theta_W M_W \cos \beta} \\ & \left. + Z_L^{2J*} Z_L^{6J} Z_N^{1i*} (Z_N^{1i*} \sin \theta_W + Z_N^{2i*} \cos \theta_W) \frac{m_{\chi_i^0} \sin \theta_W H_4(y_{Ji})}{m_\tau \cos^2 \theta_W} \right], \quad (118) \end{aligned}$$

where in the convention of [40]  $Z_+$  and  $Z_-$  are the chargino mixing matrices,  $Z_N$  is the neutralino mixing matrix,  $Z_L$  is the lepton mixing matrix,  $Z_\nu = U_D$  is the sneutrino mixing matrix and

$$x_{Ji} = \frac{m_{\tilde{\nu}_J}^2}{m_{\chi_i^+}^2}, \quad y_{Ji} = \frac{m_{\tilde{l}_J}^2}{m_{\chi_i^0}^2}. \quad (119)$$

The loop functions are given by:

$$\begin{aligned} H_1(x) &= \frac{1 - 6x + 3x^2 + 2x^3 - 6x^2 \ln x}{12(x-1)^4} \\ H_2(x) &= \frac{-1 + 4x - 3x^2 + 2x^2 \ln x}{2(x-1)^3} \\ H_3(x) &= \frac{-2 - 3x + 6x^2 - x^3 - 6x \ln x}{12(x-1)^4} \\ H_4(x) &= \frac{1 - x^2 + 2x \ln x}{2(1-x)^3} \end{aligned} \quad (120)$$

Neglecting left-right mixing in the slepton sector, the rotation matrix is given as

$$Z_L = \begin{pmatrix} U_D^* & 0 \\ 0 & V_{\text{CKM}}^\top \end{pmatrix}. \quad (121)$$

From this we can read off that in the neutralino contribution the two terms proportional to  $Z_L^{2J*} Z_L^{3J} \approx U_D^{2J} U_D^{3J*}$  dominates whereas the terms  $\propto Z_L^{2J*} Z_L^{6J}$  need LR-mixing.

#### 4.4 The neutral Higgs mass

Another observable that is quite restrictive for the CMM model is the mass of the lightest neutral, CP-even Higgs boson of the MSSM. At tree level its mass is bounded from above by the  $Z$  boson mass. However, radiative corrections shift the mass to higher values. An approximate formula at  $\mathcal{O}(\alpha\alpha_s)$  is given by [67]

$$\begin{aligned} M_h^2 &= M_h^{2,\text{tree}} + \frac{3}{2} \frac{G_F \sqrt{2}}{\pi^2} \frac{\overline{m}_t^4}{\pi^2} \left\{ -\ln \left( \frac{\overline{m}_t^2}{M_S^2} \right) + \frac{|X_t|^2}{M_S^2} \left( 1 - \frac{|X_t|^2}{12M_S^2} \right) \right\} \\ &\quad - 3 \frac{G_F \sqrt{2} \alpha_s \overline{m}_t^4}{\pi^3} \left\{ \ln^2 \left( \frac{\overline{m}_t^2}{M_S^2} \right) + \left[ \frac{2}{3} - 2 \frac{|X_t|^2}{M_S^2} \left( 1 - \frac{|X_t|^2}{12M_S^2} \right) \right] \ln \left( \frac{\overline{m}_t^2}{M_S^2} \right) \right\}, \end{aligned} \quad (122)$$

where

$$X_t = -\frac{A_t}{y_t} - \frac{\mu^*}{\tan \beta}, \quad (123)$$

$\overline{m}_t = 165 \pm 2$  GeV is the  $\overline{\text{MS}}$  mass of the top quark and

$$M_S^2 = \sqrt{m_{q_3}^2 m_{u_3}^2}. \quad (124)$$

The tree level Higgs mass is given by

$$M_h^{2,\text{tree}} = \frac{1}{2} \left[ M_A^2 + M_Z^2 - \sqrt{(M_A^2 + M_Z^2)^2 - 4M_Z^2 M_A^2 \cos^2(2\beta)} \right] \quad (125)$$

where the mass of the CP odd Higgs boson can be computed by:

$$M_A^2 = \frac{m_{H_u}^2 - m_{H_d}^2}{\cos(2\beta)} - M_Z^2 \quad (126)$$

The experimental lower bound (for large  $\tan\beta$ ) is  $M_h^{\text{exp}} \geq 89.8$  GeV [50]. Since the coupling strength of the  $Z$  boson to  $h^0$  depends on the MSSM Higgs mixing angles, especially on  $\sin(\beta - \alpha)$ , the experimental lower bound for small  $\tan\beta$ , relevant for our analysis, is close to the Higgs mass bound in the SM [68]:

$$M_h^{\text{exp}} \geq 114.4 \text{ GeV} \quad (127)$$

In the next section we will see that for  $\tan\beta = 3$  the constraints from the lightest Higgs mass are much more stringent than the FCNC bounds. This is due to the fact that the large top Yukawa coupling drives the masses of the third squark generation to smaller values such that the corrections to the tree level Higgs mass cannot compensate for the difference between  $M_h^{\text{tree}}$  and the experimental lower bound.

#### 4.5 Further experimental input parameters

For our analysis we used the following experimental input :

$$\begin{array}{ll} \alpha_e(M_Z) = 1/128.129 & [69, 70] \\ \alpha_s(M_Z) = 0.1184 & [71] \\ M_W = 80.398 \text{ GeV} & [50] \\ M_Z = 91.1876 \text{ GeV} & [50] \\ m_\tau = 1.777 \text{ GeV} & [50] \end{array} \quad \begin{array}{ll} \sin^2 \theta_W = 0.23138 & [50, 69] \\ G_F = 1.16637 \times 10^{-5} \text{ GeV}^{-2} & [50] \\ m_t = 173.3 \text{ GeV} \text{ (pole mass)} & [72] \\ m_b(m_b) = 4.163 \text{ GeV} & [73] \\ m_b = 4.911 \text{ GeV} \text{ (pole mass)}. & \end{array}$$

The pole mass of the bottom quark was obtained using the above value for  $m_b(m_b)$  and the program RunDec [74].

For the MNS matrix we use the tri-bimaximal mixing [75], i.e. a parametrization with  $\theta_{12} = 30^\circ$ ,  $\theta_{23} = 45^\circ$ , and  $\theta_{13} = 0^\circ$ . The CKM matrix is constructed via the Wolfenstein parametrization [76] using the latest parameters from the CKMfitter group [77]:

$$\begin{aligned} \lambda &= 0.22543 \\ A &= 0.812 \\ \bar{\rho} &= 0.144 \\ \bar{\eta} &= 0.342. \end{aligned} \quad (128)$$

## 5 Results

The correlation of observables in Sec. 4 allows us to constrain the parameter space of the CMM model. In order to test the model, we first choose a scenario in which the specific signatures of

the model are enhanced and flavor-violating effects are maximal: As discussed in Sec. 3.1 with  $\tan\beta = 3$  the top Yukawa coupling is near its infrared fixed point such that the mass splitting between the first two generations and the third one is maximal without losing the perturbativity of  $y_t$ . The rotation into the super-CKM basis (see Eq. (21)) translates this into maximal flavor violation. Whereas the FCNC constraints still allow some regions in the CMM model parameter space, the model is challenged by the experimental lower bound on the Higgs mass. However, this can be reconciled in a relaxed scenario with  $\tan\beta = 6$ . We discuss both the  $\tan\beta = 3$  and the  $\tan\beta = 6$  cases. In the first case we get maximal effects in the flavor sector, because of the large intergenerational squark mass splitting. In this scenario we explore the viable parameter space of the CMM model. If we find that the model is not excluded, then this will also be true for larger values of  $\tan\beta$ . The  $\tan\beta = 6$  case corresponds to a consistent scenario. We further take  $\mu$  real to avoid problems with electric dipole moments.

### Vacuum stability and positive soft bilinear terms

Since the trilinear  $A$ -terms can lead to charge- and color-breaking minima of the scalar potential, the CMM input parameter  $a_1^d$  is restricted to fulfill the stability bound [78]

$$\left|a_1^d(M_Z)\right| < \sqrt{3 \left(m_{\tilde{q}_1}^2 + m_{\tilde{d}_1}^2 + m_{H_d}^2\right)}. \quad (129)$$

We have checked that in our parameter scan with  $|a_1^d|/M_{\tilde{q}} < 3$  this condition is satisfied almost everywhere. Similarly, we must exclude unphysical regions with negative soft squared masses of sfermions carrying  $U(1)_{\text{em}}$  or  $SU(3)_C$ -charges which can occur if  $y_t$  drives the third-generation sfermion masses to negative values at the electroweak scale. This limits the mass splitting and thus the size of flavor-violating effects. In the following plots the black regions are unphysical due to  $m_{\tilde{f}}^2 < 0$  or an unstable vacuum. The actual experimental lower bounds on the masses have no relevant effect. This is due to the fact that close to the negative mass bound, the soft masses decrease from typical masses of  $\mathcal{O}(M_{\text{SUSY}})$  to zero quite rapidly. This happens in intervals of  $M_{\tilde{q}}$  and  $a_1^d$  that are really small as compared to the intervals we are scanning over. Therefore we will not distinguish between the negative soft mass bounds and the bounds resulting of sfermion masses falling below their experimental lower bounds.

### Mass splitting

The CMM model specific flavor effects are crucially determined by the mass splitting of the right-handed down squarks (see Eq. (21)). In Fig. 3 the relative mass splitting  $\Delta_d^{\text{rel}} = 1 - m_{\tilde{d}_3}^2/m_{\tilde{d}_2}^2$  is shown. In Figs. 3–5 we depict the quantities of interest as contour plots in a the  $M_{\tilde{q}}$ - $a_1^d/M_{\tilde{q}}$  plane. Here the mass of the right-handed squarks of the first two generations,  $M_{\tilde{q}}$ , (which is essentially degenerate with the masses of the corresponding left-handed masses) and the trilinear term  $a_1^d$  are defined at the low scale  $Q = M_Z$ . In the plots we further use  $m_{\tilde{g}_3}(M_Z) = 500$  GeV,  $\text{sgn } \mu = +1$ ,  $\tan\beta = 3$  (left) and  $\tan\beta = 6$  (right). The mass splitting increases with  $|a_1^d(M_Z)|/M_{\tilde{q}}(M_Z)$  and decreases as expected with  $\tan\beta$ . For a heavier gluino mass the allowed physical region moves to larger values of  $M_{\tilde{q}}(M_Z)$  and changing the sign of  $\mu$  does not have any significant effect.



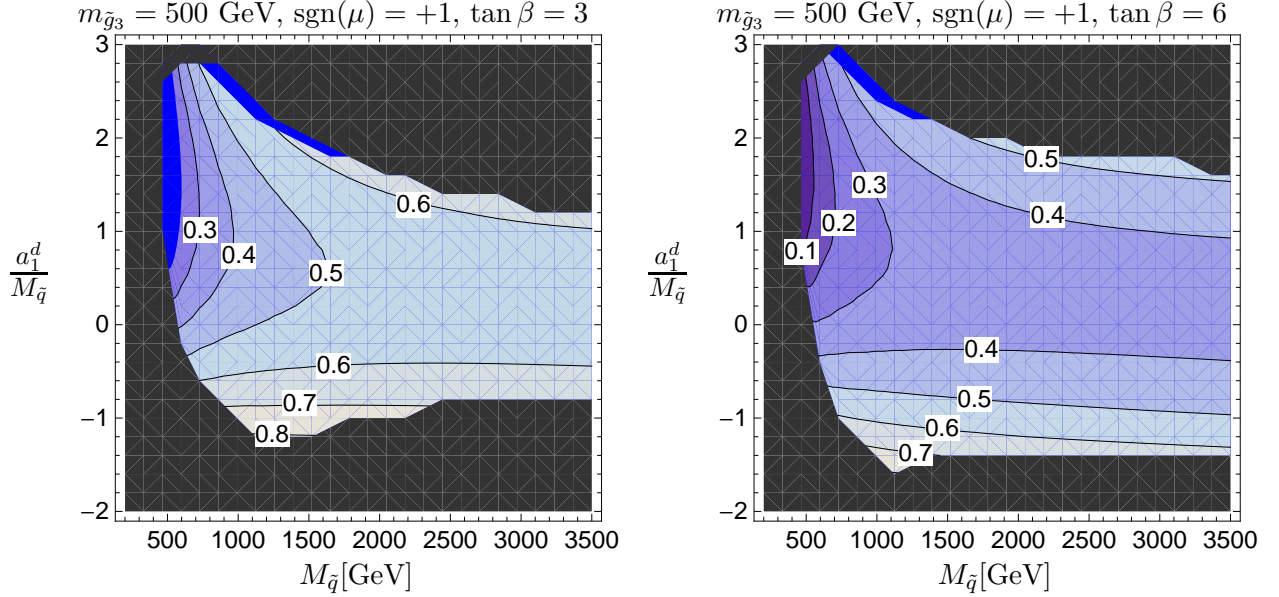


Figure 3: Relative mass splitting  $\Delta_d^{\text{rel}} = 1 - m_{d3}^2/m_{d2}^2$  among the bilinear soft terms for the right-handed squarks of the second and third generations with  $\tan \beta = 3$  (left) and 6 (right) in the  $M_{\tilde{q}}(M_Z) - a_1^d(M_Z)/M_{\tilde{q}}(M_Z)$  plane for  $m_{\tilde{g}_3} = 500$  GeV and  $\text{sgn}(\mu) = +1$ .

### Sparticle spectrum and FCNC observables for a specific parameter point

Exemplarily, we present the output for one CMM model parameter point. We choose the same inputs as in Sec. 3.7 where the parameters at the GUT scale have been discussed:

$$M_{\tilde{q}} = 1500 \text{ GeV}, \quad m_{\tilde{g}_3} = 500 \text{ GeV}, \quad a_1^d/M_{\tilde{q}} = 1.5, \quad \arg(\mu) = 0, \quad \tan \beta = 6. \quad (130)$$

The sparticle spectrum at the electroweak scale is given as (mass eigenvalues):

$$m_{\tilde{g}_1} = 83 \text{ GeV}, \quad m_{\tilde{g}_2} = 165 \text{ GeV}, \quad (131)$$

$$m_{\tilde{\chi}_i^0} = (640, 632, 159, \underline{81}) \text{ GeV} \quad (132)$$

$$m_{\tilde{\chi}_i^\pm} = (640, 159) \text{ GeV} \quad (133)$$

$$M_{\tilde{t}_i} = (1427, 1427, \mathbf{1074}, 1462, 1462, \mathbf{1095}) \text{ GeV} \quad (134)$$

$$M_{\tilde{u}_i} = (1519, 1519, \mathbf{934}, 1501, 1501, \mathbf{485}) \text{ GeV} \quad (135)$$

$$M_{\tilde{d}_i} = (1519, 1519, \mathbf{908}, 1498, 1498, \mathbf{1164}) \text{ GeV}. \quad (136)$$

The lightest neutralino is identified as the LSP (underlined number). The first three entries in  $M_{\tilde{f}_i}$ ,  $\tilde{f} = \tilde{l}, \tilde{u}, \tilde{d}$  correspond to sfermions with a larger left-handed component and the last three with a larger right-handed component, where the third generation masses are printed in bold face. The typical mass splitting is quite evident. The mixing angle between the two stop eigenstates with 485 GeV and 934 GeV is  $\theta_{\tilde{t}} = 11^\circ$  and left-right mixing in the down sector is negligible, owing to the small value of  $\tan \beta$ . While  $M_{d_4}^2 = M_{d_5}^2 = m_{d_1}^2 = m_{d_2}^2$ , the flavor composition of the two

eigenstates  $\tilde{d}_4$  and  $\tilde{d}_5$  is very different:  $\tilde{d}_4$  is the right-handed down squark, while  $\tilde{d}_5$  (like  $\tilde{d}_6$ ) is a maximal mixture of right-handed sstrange and sbottom. We here observe a generic feature of models in which  $y_t$  is the only driver of non-universal soft squark masses: Since the unitary rotation transforming the squark mass matrix to diagonal form preserves the eigenvalues, the degeneracy in Eq. (20) persists in the spectrum in Eq. (136) as  $M_{\tilde{d}_4} = M_{\tilde{d}_5}$ . The Higgs parameters read:

$$m_{H_u}^2 = -(575 \text{ GeV})^2, \quad m_{H_d}^2 = (1432 \text{ GeV})^2, \quad \mu = 629 \text{ GeV}. \quad (137)$$

This fulfills the condition for electroweak symmetry breaking. The trilinear terms are given as:

$$\hat{A}_u = \begin{pmatrix} 0 & 0 & 0 \\ 0 & 0 & 0 \\ 0 & 0 & 46.9 \end{pmatrix} \text{ GeV}, \quad \hat{A}_d = \begin{pmatrix} 0 & 0 & 0 \\ 0 & 0 & 0 \\ 0 & 0.5 - 0.8i & -14.1 \end{pmatrix} \text{ GeV}, \quad \hat{A}_\ell = \begin{pmatrix} 0 & 0 & 0 \\ 0 & 0 & 0.3 - 0.4i \\ 0 & 0 & -5.9 \end{pmatrix} \text{ GeV}. \quad (138)$$

For the radiative decays we obtain

$$\mathcal{B}(\tau \rightarrow \mu\gamma) = 1.66 \cdot 10^{-8} \quad \text{and} \quad \mathcal{B}(b \rightarrow s\gamma) = 2.89 \cdot 10^{-4} \quad (139)$$

where the latter is just above the lower end of the allowed  $3\sigma$  region. Omitting the (3,2) entry of  $\hat{A}_d$  would lead to an increase of  $\mathcal{B}(b \rightarrow s\gamma)$  of about  $0.03 \cdot 10^{-4}$  for this particular parameter point. Note, however, that for smaller gluino masses and e.g.  $\tan\beta = 3$  effects of up to  $0.7 \cdot 10^{-4}$  can be ascribed to the presence  $\hat{A}_{d,3,2}$ . This effect was not considered in previous analyses.

We determine the phase  $\xi$  such that it leads to values of  $\Delta M_s$ ,  $\sin\phi_s$  and  $f_{B_s}\sqrt{\hat{B}_{B_s}}$  that are as close as possible to their experimental and theoretical values, respectively, by minimizing the  $\chi^2$  for  $\Delta M_s$ ,  $\sin\phi_s$  and  $f_{B_s}\sqrt{\hat{B}_{B_s}}$ . To this end we scan over the theoretical error of  $f_{B_s}^2\hat{B}_{B_s}$  (see Eq. (73)), the experimental region for  $\sin\phi_s$  (see Eq. (87)) and  $\Delta M_s$ . As a best fit value for the chosen parameter point, we obtain the phase  $\xi = 58^\circ$ , yielding  $\Delta M_s = 17.68 \text{ ps}^{-1}$  and  $f_{B_s}\sqrt{\hat{B}_{B_s}} = 0.260 \text{ GeV}$ . This corresponds to a phase  $\phi_s = -49^\circ$  meaning  $\sin\phi_s = -0.75$ . Alternatively, we can also ignore the experimental value of  $\sin\phi_s$  and simply ask the question how large  $\phi_s$  can become for the parameter point in Eq. (130), given the experimental and theoretical regions for  $\Delta M_s$  and  $f_{B_s}\sqrt{\hat{B}_{B_s}}$ . In this case,  $\xi$  can be adjusted such that the maximally allowed (negative) phase reads  $\phi_s = -52^\circ$ . The same basic procedure is also applied in the following analysis.

## Correlation of observables

A combination of the flavor observables described in Sec. 4 restricts the CMM parameter space. This is illustrated in Fig. 4 where we distinguish again between  $\tan\beta = 3$  and  $\tan\beta = 6$ . The green region is still compatible with  $B_s - \bar{B}_s$ ,  $b \rightarrow s\gamma$  and  $\tau \rightarrow \mu\gamma$ . For larger gluino mass the allowed area increases. Furthermore, the qualitative behavior for negative  $\mu$  does not change. In this case,  $\tau \rightarrow \mu\gamma$  together with  $B_s - \bar{B}_s$  leads to the strongest constraints. Because of decoupling the green region increases with the SUSY scale. Furthermore we find that in the parameter space where the CMM model could be valid, the lightest supersymmetric particle is almost everywhere the lightest neutralino.

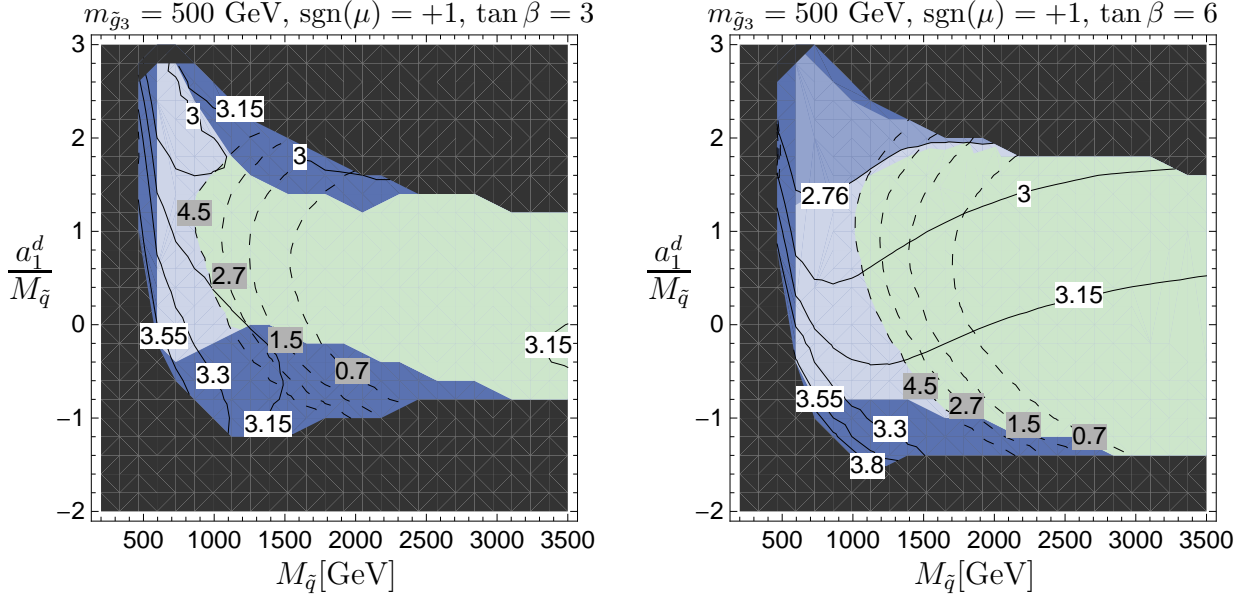


Figure 4: Correlation of FCNC processes as a function of  $M_{\tilde{q}}(M_Z)$  and  $a_1^d(M_Z)/M_{\tilde{q}}(M_Z)$  for  $m_{\tilde{g}_3}(M_Z) = 500$  GeV and  $\text{sgn } \mu = +1$  with  $\tan \beta = 3$  (left) and  $\tan \beta = 6$  (right).  $\mathcal{B}(b \rightarrow s\gamma)[10^{-4}]$  solid lines with white labels;  $\mathcal{B}(\tau \rightarrow \mu\gamma)[10^{-8}]$  dashed lines with gray labels. Black region:  $m_{\tilde{f}}^2 < 0$  or unstable  $|0\rangle$ ; dark blue region: excluded due to  $B_s - \overline{B}_s$ ; medium blue region: consistent with  $B_s - \overline{B}_s$  but excluded due to  $b \rightarrow s\gamma$ ; light blue region: consistent with  $B_s - \overline{B}_s$  and  $b \rightarrow s\gamma$  but inconsistent with  $\tau \rightarrow \mu\gamma$ ; green region: compatible with all three FCNC constraints.

What is really challenging for the CMM model is an observable not directly related to flavor physics: the mass of the lightest neutral, CP-even Higgs boson. As already mentioned at the end of Sec. 4, in order to make the corrections to the tree level Higgs mass large enough, the sfermions of the third generation should not be too light because they enter together with the top mass logarithmically in the radiative corrections (see Eq. (122)). This is triggered by the choice of  $\tan \beta$ . In Fig. 5 one can see the same parameter space as in Fig. 4 but with the predicted mass of the lightest Higgs boson mass added (solid line with white labels). On the left hand side for  $\tan \beta = 3$  the whole green region is excluded due to  $M_{h^0} < 114.4$  GeV. For negative  $\mu$  the mass even tends to smaller values. Only for rather heavy masses, e.g.  $m_{\tilde{g}_3} = 2500$  GeV and  $M_{\tilde{q}} \gtrsim 6500$  GeV the experimental bound can be satisfied. However, in this region of parameter space the constraints from flavor violating processes become irrelevant. On the right hand side of Fig. 5 for  $\tan \beta = 6$  the situation changes such that even for light gluino masses there exist allowed regions in the CMM parameter space. Thus, we can summarize this correlation between flavor violation and Higgs mass in the CMM-model:

small $\tan \beta$	$\Leftrightarrow$	large flavor effects	$\Leftrightarrow$	(too) light $h^0$
larger $\tan \beta$	$\Leftrightarrow$	smaller flavor effects	$\Leftrightarrow$	sufficiently heavy $h^0$

In light of the recent result from DØ of the like-sign dimuon charge asymmetry and the measured CP violation in  $B_s \rightarrow J/\psi\phi$ , it is worth studying how large the CP phase  $\phi_s$  can actually be in

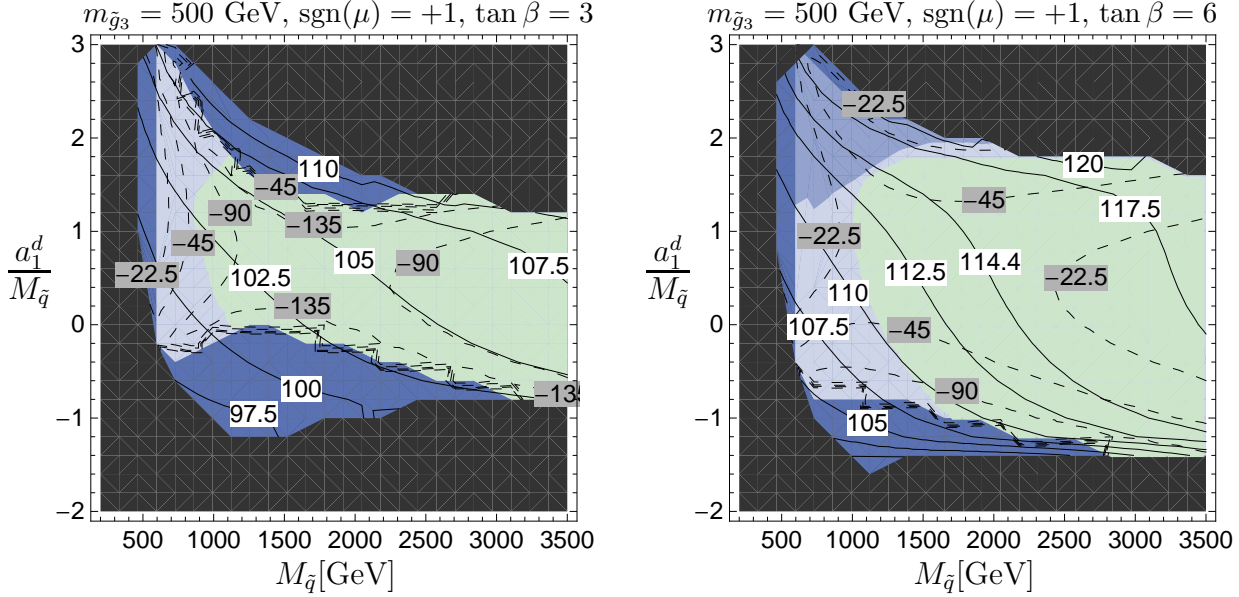


Figure 5: Same as in Fig. 4, but without labels and lines for  $b \rightarrow s\gamma$  and  $\tau \rightarrow \mu\gamma$ . We show the lightest Higgs mass in GeV (solid line with white labels) and the phase  $\phi_s$  in degrees (gray labels) for  $\tan \beta = 3$  (left) and  $\tan \beta = 6$  (right).  $\phi_s$  depends on the CP phase  $\xi$  of the model; the values quoted in the gray labels are the values of  $\phi_s$  with maximal possible  $|\phi_s|$ .

the CMM model. It is related to the free phase  $\xi$  defined in Eq. (21) which occurs in the Wilson coefficient (see Eq. (77)) of the  $B_s - \bar{B}_s$  system. In Fig. 5 we also compute the maximal (negative) phase  $\phi_s$  in the CMM model under the condition that  $\Delta M_s$  lies within its  $3\sigma$ -range and the hadronic matrix element within its error bar.

From Fig. 4 we see that  $\tau \rightarrow \mu\gamma$  alone puts a lower bound on  $M_{\tilde{q}}$ , so that the squark masses of the first two generations lie essentially above 1 TeV. One also realizes that the bound on  $\mathcal{B}(\tau \rightarrow \mu\gamma)$  is more constraining than the measured value of  $\mathcal{B}(b \rightarrow s\gamma)$ . Fig. 3 shows that the dominantly right-handed sbottom is about half as heavy as the down-type squarks of the first two generations. The sample parameter point discussed in Eqs. (130–136) further shows that we can expect a dominantly right-handed stop with mass around 500 GeV. The sleptons are heavy and seemingly out of the discovery range of the LHC. On the other hand, the light gaugino-like chargino and neutralinos should permit nice signatures in the “golden” triplepton search channels. Fig. 5 reveals that the lower bound on the lightest neutral Higgs boson mass excludes the whole plotted region if  $\tan \beta = 3$ . In the  $\tan \beta = 6$  case this bound has a much milder effect, essentially leading to a preference of the upper half of the plotted region, where  $a_1^d > 0$ . Remarkably, almost all of the allowed region permits large effects in  $B_s - \bar{B}_s$  mixing, with CP phases well in the range needed to explain the Tevatron data and quoted in Eq. (87). That is,  $B_s - \bar{B}_s$  mixing is much more sensitive to the new physics effects than the rare decays entering our analysis. The light gauginos are, of course, a consequence of our choice of  $M_{\tilde{g}} = 500 \text{ GeV}$  in our numerical studies. We may ask how the patterns of Figs. 3–5 change, if  $M_{\tilde{g}}$  is increased. In particular, one might expect that the FCNC constraints become

weaker so that one could instead obtain lighter squarks of the first two generations. However, this is not the case, instead the lower bound on  $M_{\tilde{q}}$  becomes stronger with increasing  $M_{\tilde{g}}$ , in order to avoid too light third-generation squarks and problems with  $\Delta M_s$ .

We conclude that in the CMM model it is indeed possible to explain the observed discrepancies in the  $B_s$  system naturally with the free phase  $\xi$  and simultaneously satisfy other FCNC bounds. Compared to the generic MSSM that can also describe CP violation in  $B_s - \bar{B}_s$  mixing, but does not suppress FCNC elsewhere, the CMM model in its original formulation does not induce any dangerous effects in e.g. Kaon mixing or  $\mu \rightarrow e\gamma$  due to the smallness of  $(U_{\text{PMNS}})_{13}$  which translates into the particular structure of the right-handed down squark mass matrix in Eq. (21). By contrast, the generic MSSM lacks a symmetry principle that governs the structure of the squark mass matrices in a way which suppresses  $b \rightarrow d$ ,  $s \rightarrow d$  and  $c \rightarrow u$  transitions while permitting large CP-violating effects in  $b \rightarrow s$  transitions. Note, that there are also some effects in  $\Delta B = 1$  penguin diagrams such as  $B_d \rightarrow \phi K_S$  and  $B_s \rightarrow \phi\phi$ , which triggered the early studies in [18] and [22]. The experimental value of  $\Delta M_s$  restricts the size of the new physics contribution to  $M_{12}^s$  to smaller values than those allowed before the discovery of  $B_s - \bar{B}_s$  mixing. In the portion of the CMM parameter space complying with all of today's experimental constraints the contribution to CP asymmetries in  $b \rightarrow s$  penguin decays is small and typically in a range which cannot be resolved within present experimental errors. We will discuss the impact of the CMM model on these CP asymmetries in the light of future experimental uncertainties in another paper.

## 6 Comparison with other GUT analyses

In the following we compare the CMM model and our results with analyses of other authors.

Moroi's landmark papers [10] have laid out the basic idea of the CMM model, namely flavor violation in the soft squark mass terms driven by RG evolution above the GUT scale in conjunction with large lepton-flavor violation. The paper discusses the effect in an SU(5) context and focuses on the phenomenological effects in  $B_d - \bar{B}_d$  mixing and CP violation in  $b \rightarrow s$  penguin decays. Written prior to the  $B$  factory era, the author mentions the possibility of new CP phases in  $b \rightarrow s$  penguin decays of order  $5^\circ$ . The consequences of a large top Yukawa coupling (studied in minimal SU(5) and SO(10) models) in conjunction with universal soft terms at  $M_{\text{Pl}}$  for low-energy flavor observables have already been studied by Barbieri et al. in 1995 [14]. In this paper the non-degeneracy of third-generation fermions with the first and second generation is emphasized. Since [14] has been written at a time at which the neutrino mixing matrix was unknown, the phenomenological results cannot be compared to ours in a meaningful way. Harnik et al. have analyzed the  $b \rightarrow s$  penguin amplitude in a framework inspired by the CMM model [18]: Motivated by a  $2.7\sigma$  discrepancy between the measured mixing-induced CP asymmetry in  $B_d^0 \rightarrow \phi K_S$  and the SM expectation, they have supplemented the MFV-MSSM by a  $\tilde{b}_R - \tilde{s}_R$  mixing term determined by the atmospheric neutrino mixing angle. Since no RG analysis has been worked out, the authors could not find the correlations between the various observables and the sparticle spectrum, which originates from the small number of GUT parameters and is presented in the preceding section. However, correlations among  $B_s - \bar{B}_s$  mixing,  $b \rightarrow s\gamma$  and CP violation in  $B_d \rightarrow \phi K_S$  stemming from the  $\tilde{b}_R - \tilde{s}_R$  off-diagonal element of the squark mass matrix are already studied in [18], scanning over MSSM

parameters. The authors of [18] also discuss the possibility that the  $\tilde{b}_R - \tilde{s}_R$  and  $\tilde{b}_R - \tilde{b}_L$  mixings are simultaneously large. We do not see how this can be achieved even in a widely defined class of CMM-like models: A large  $\tilde{b}_R - \tilde{b}_L$  mixing amounts to a large value of  $m_b \mu \tan \beta$  and therefore inevitably to a sizable  $\tan \beta$  ( $|\mu|$  is fixed from the condition of electroweak symmetry breaking) and the corresponding smaller value of  $y_t$  quickly renders the PMNS-driven  $\tilde{b}_R - \tilde{s}_R$  mixing small, see Fig. 2. In [22] two authors of this paper have analyzed  $B_s - \bar{B}_s$  mixing in conjunction with  $\tau \rightarrow \mu\gamma$  in the CMM model as defined in this paper performing an RG analysis which has not yet included the MSSM Higgs sector (and the constraint from  $m_{h^0}$ ) and  $b \rightarrow s\gamma$ . Both [18] and [22] found order-of-magnitude enhancements of  $\Delta M_{B_s}$  (which was unknown at the time) over the SM prediction in those regions of the parameter space explaining the experimental anomaly in  $B_d \rightarrow \phi K_S$  seen at the time. This merely reflects the larger sensitivity of  $B_s - \bar{B}_s$  mixing to  $\tilde{b}_R - \tilde{s}_R$  mixing compared to  $b \rightarrow s$  penguin amplitudes.

Among the papers studying GUT flavor physics in a SUSY SU(5) context, [13] has a significant overlap with our analysis: In [13] also universal scalar masses and trilinear  $A$ -terms are postulated at the reduced Planck scale and the PMNS matrix appears in the RGE of the right-handed down squarks. Like us, the authors of [13] study  $\tau \rightarrow \mu\gamma$ ,  $b \rightarrow s\gamma$  and  $\phi_s$ , but with focus on the mixing-induced CP asymmetry in  $B_d \rightarrow \phi K_S$ . The study goes beyond ours by considering the electric dipole moment of the muon and CP violation in  $B_d^0 \rightarrow M_s^0 \gamma$ . Values of  $\tan \beta$  up to 30 are considered, which are inaccessible in the CMM model. In a recent phenomenological update [52] the authors of [13] have calculated  $|\phi_s|$  in their SU(5) model and found a maximal value of  $9^\circ$ . This is in sharp contrast to the situation found by us in the CMM model. The work [51] also studies the possibility that in SUSY GUT models with heavy right-handed neutrinos the large atmospheric mixing angle can affect  $b \rightarrow s$  transitions due to a large Dirac neutrino Yukawa coupling (which in our case is equal to the top Yukawa coupling). Using the mass insertion approximation, the correlation of new physics effects in  $B_q - \bar{B}_q$ -mixing ( $q = d, s$ ) and the radiative decays  $\tau \rightarrow e(\mu)\gamma$  is discussed. In contrast to our work, the GUT model is not specified and a detailed renormalization group analysis is missing. Employing the approximate GUT relation  $\delta_{RR}^{dij} \approx \delta_{LL}^{\ell ij}$  (which is not necessarily true with large mixing and is not invariant under the RG) the ratio of the  $B_d$  and  $B_s$  mixing frequencies is correlated to the corresponding ratio of the LFV decays  $\tau \rightarrow e(\mu)\gamma$ . In [53] the RG-induced flavor violation is studied in conjunction with dimension-5 Yukawa terms and the corresponding soft SUSY-breaking terms. These papers find that given the constraint from  $\mathcal{B}(\tau \rightarrow \mu\gamma)$  the impact on  $B_s - \bar{B}_s$  mixing is maximal for a particular value of the ratio  $m_{\tilde{g}}/m_0$  around 0.3. Our sample point discussed in Sec. 3.7 is in qualitative agreement with this finding. LFV decays are also correlated with quark FCNC processes in various SU(5) and SO(10) scenarios in [79]. The authors discuss several ansätze to alleviate different tensions in quark FCNC data. As an important difference with respect to the CMM model the scenarios of [79] contain relevant sources of flavor symmetry breaking among the first two fermion generations, so that e.g.  $\mathcal{B}(\mu \rightarrow e\gamma)$  places a constraint on the parameter spaces. Recently Buras et al. have presented a correlated analysis of many flavor observables in an SU(5) scenario with right-handed neutrinos [54] and mSUGRA boundary conditions at  $M_{\text{Pl}}$ . The Yukawa sector is less constrained than in the CMM model and therefore the correlations between different FCNC observables are weaker. Like us and in contrast to [52], the authors of [54] find that the current upper bound on  $\mathcal{B}(\tau \rightarrow \mu\gamma)$  still permits a sizable

CP phase in  $B_s - \bar{B}_s$  mixing. In [54] also FCNC transitions among the first and second generation are studied, e.g.  $K - \bar{K}$  mixing and  $\mu \rightarrow e\gamma$ . This procedure is not in our philosophy, because these transitions are highly sensitive to corrections from higher-dimensional operators, which are moreover welcome to fix the poor Yukawa unification in the first two generations. Our approach, pursued in two previous papers, is to constrain the flavor structures of higher-dimensional operators from data on  $K - \bar{K}$  mixing [38] and  $\mu \rightarrow e\gamma$  [39].

There are numerous papers on the MSSM with GUT boundary conditions placed at  $M_{\text{GUT}}$ . These papers are different in spirit to [10, 12–14, 18, 22, 51, 52, 54] and this paper, all of which employ RG effects above  $M_{\text{GUT}}$ . Here we discuss two of these papers with particular emphasis on flavor physics: In [80] correlations of quark and lepton FCNCs are studied in SU(5) SUSY GUTs, but without neutrinos (and thus without the PMNS matrix). The authors of [80] assume generic flavor-violating entries to be present in the sfermion matrices at the GUT scale and correlate quark and lepton FCNCs in a general way via SU(5) symmetry. Using the mass insertion approximation, an upper bound for the off-diagonal elements of the right-handed down squark matrix of the form  $|\delta_{RR}^{dij}| \leq \frac{m_L^2}{m_D^2} \delta_{LL}^{\ell ij}$  has been derived. The authors have found that the bound on  $\delta_{RR}^{d23}$  induced by  $\tau \rightarrow \mu\gamma$  is stronger than those from the  $B$  physics observables known at the time. The authors of [81] have studied an SO(10) SUSY GUT model with  $D_3$  family symmetry which was proposed in [82]. This model involves Yukawa unification of the third generation at the GUT scale, which immediately implies large  $\tan\beta \approx 50$  at low energies. This is already in sharp contrast to the CMM model where  $y_b$  is suppressed by a factor  $\langle 45_H \rangle / M_{\text{Pl}}$  compared to  $y_t$  and the phenomenology is very different. With 24 input parameters, all parameters at low energy (including SM parameters) can be calculated with the RGE and it is possible to get realistic quark and lepton masses as well as the PMNS and CKM matrix. The authors have a closer look at their SUSY spectrum and study FCNC processes like  $B_s \rightarrow \mu^+\mu^-$ ,  $B \rightarrow X_s\gamma$ ,  $B \rightarrow X_s\ell^+\ell^-$  and  $\Delta M_{d,s}$  and the decay  $B^+ \rightarrow \tau^+\nu$ . The combination of these observables is challenging for the model, since mass hierarchies enter loops in FC observables. The authors conclude that this problem occurs in a wider class of SUSY GUTs with unified Yukawa couplings of the third generation. This argument, which was further pursued in [83], is, however, not applicable to the CMM model.

## 7 Conclusions

We have studied a supersymmetric SO(10) GUT model originally proposed by Chang, Masiero and Murayama (CMM model) [12], in which the large atmospheric neutrino mixing angle  $\theta_{23}$  is transferred to  $b \rightarrow s$  and  $\tau \rightarrow \mu$  transitions. At low energy the model is an MSSM whose parameters are highly correlated through the GUT boundary conditions. The key features of the CMM model are soft SUSY-breaking terms which are universal near the Planck scale and a Yukawa sector with a non-renormalizable term in the SO(10) superpotential as the only source of flavor violation. Renormalization-group effects of the large top Yukawa coupling  $y_t$  drive the sfermion masses of the third generation away from those of the first two generations. The transition from weak to mass eigenstates involves rotations with the atmospheric mixing angle among right-handed bottom and strange squarks and left-handed tau and muon sleptons. This leads to potentially large FCNC effects in transitions between the second and third generation, while other FCNC transitions are essentially

unaffected. We have performed an extensive RGE analysis to connect Planck-scale and low-energy parameters, focusing on the numerically dominant effects associated with the large parameters  $y_t$  and  $\theta_{23} \simeq 45^\circ$ .

We have then analyzed the FCNC observables  $\mathcal{B}(\tau \rightarrow \mu\gamma)$ ,  $\mathcal{B}(b \rightarrow s\gamma)$ , the mass difference  $\Delta M_s$  in  $B_s-\bar{B}_s$  mixing, and the corresponding CP phase  $\phi_s$ , taking into account the LEP lower bound on the lightest neutral Higgs boson mass  $m_{h^0}$ . The analysis involves only seven new parameters, so that the model is very predictive. We find that  $\tau \rightarrow \mu\gamma$  constrains the sfermion masses of the first two generations to lie above 1 TeV, while the third-generation sfermions can be substantially lighter. The intergenerational sfermion mass splitting is larger than in models which impose universal soft terms at the GUT scale, such as the CMSSM. At the same time the CMM model permits light gauginos.  $b \rightarrow s\gamma$  is less constraining than  $\tau \rightarrow \mu\gamma$ , while  $B_s-\bar{B}_s$  mixing turns out to be most sensitive to CMM effects. One of the model parameters is a CP-violating phase accompanying  $\tilde{b}_R \rightarrow \tilde{s}_R$  transitions and we can accommodate the recent hints for new physics in  $B_s-\bar{B}_s$  mixing [55].

We find that the LEP bound  $m_{h^0} \geq 114.4$  GeV places a powerful constraint on the parameter space of the CMM model: E.g. for  $\tan\beta = 3$  the sfermion masses must be unnaturally high to comply with  $m_{h^0} \geq 114.4$  GeV, which in turn does not permit visible effects in the FCNC observables. However, for  $\tan\beta = 6$  we find regions of the CMM parameter space compatible with all data and large effects in  $B_s-\bar{B}_s$  mixing. The pattern of sparticle masses is very distinctive: Sfermions are heavy, with the exception of a dominantly right-handed stop. Since  $y_t$  is the only source of sfermion non-universality, eight out of twelve squarks and four out of six sleptons are essentially degenerate. Most importantly, two of the physical squarks are maximal  $\tilde{b}_R-\tilde{s}_R$  mixtures and likewise two sleptons are maximal  $\tilde{\tau}_L-\tilde{\mu}_L$  mixtures. This should lead to distinctive features in the collider signatures at CMS and ATLAS.

In summary, we have performed an RG analysis of the CMM model relating several observables to seven new parameters beyond those of the standard model. We find that the model can explain the hints for a large CP phase in  $B_s-\bar{B}_s$  mixing seen in current data without violating other FCNC constraints, vacuum stability bounds or the experimental lower bounds on  $m_{h^0}$  and supersymmetric particle masses.

## Acknowledgments

The presented work is supported by project C6 of the DFG Research Unit SFB-TR 9 *Computergestützte Theoretische Teilchenphysik* and by the DFG grant No. NI 1105/1-1. J.G. and W.M. acknowledge the financial support by *Studienstiftung des deutschen Volkes*. S.J. was supported by the Science and Technology Facilities Council [grant number ST/H004661/1] and acknowledges support from the NExT institute and SEPnet.

## A Higgs Sector and Yukawa Couplings in the CMM Model

The CMM model makes use of small Higgs representations:  $\text{SO}(10)$  is broken to the standard model via the Higgs fields  $16_H$ ,  $\bar{16}_H$  and  $45_H$ . The electroweak symmetry is then broken when the neutral component in the doublet  $H_u \in 10_H$  acquires a vev. In addition to  $H_u$ , the theory contains a second



Higgs doublet,  $H_d$ , which couples to down quarks as well as charged fermions. A priori, this field can originate from two different  $\text{SO}(10)$  representations (or a combination of the two).

As discussed in Sec. 2, the adjoint Higgs field is assumed to acquire two distinct vevs. While the primary task of  $45_H$  is to break  $\text{SU}(5)$  to the standard model group, the  $\text{SU}(5)$  singlet component might acquire a vev as well when  $\text{SO}(10)$  is broken via the spinorial Higgs field.<sup>8</sup>

If  $H_d$  was contained in  $10_H$  as well, the mass and weak eigenstates would coincide and the quark mixing matrix would be the unit matrix. (Mixing among leptons could originate from the Majorana mass matrix for the right-handed neutrinos.) We therefore have to consider an additional Higgs field in the theory, which can incorporate all or part of  $H_d$ .<sup>9</sup> This case is realized in the CMM model. In order to allow for an asymmetric Yukawa coupling matrix for down quarks and charged fermions, the matter fields couple to  $10'_H$  via a non-renormalizable interaction,  $16 \ 16 \ 10'_H \ 45_H$ . As already mentioned, this higher-dimensional operator can be generated by integrating out massive  $\text{SO}(10)$  fields. Depending on the representation of the massive field, four invariants can appear [35],<sup>10</sup>

$$\begin{aligned} (16 \ 16)_{10} (10_H \ 45_H)_{10}, & \quad (16 \ 10_H)_{\overline{16}} (16 \ 45_H)_{16}, \\ (16 \ 16)_{120} (10_H \ 45_H)_{120}, & \quad (16 \ 10_H)_{\overline{144}} (16 \ 45_H)_{144}. \end{aligned} \quad (140)$$

The expressions in the right column can be expressed in terms of those in the first column through a Fierz transform. The contributions are either symmetric or antisymmetric [36], so that the effective Yukawa coupling  $Y_2$  has a mixed symmetry.

The CMM model focuses on the singlet vev,  $v_0 = \langle S(45_H) \rangle$ , for two reasons. One,  $v_0$  is an order of magnitude larger than  $\sigma$  such that the ratio  $M_{\text{Pl}}/v_0 \sim 10^1 - 10^2$  is smaller than the top-bottom mass ratio. Thus,  $\tan \beta$  can be as large as 10 with moderate values for  $Y_2$ . Two, for  $\sigma = 0$  the contributions to  $Y_d$  and  $Y_e$  from Eq. (140) satisfy relation Eq. (1) with no further symmetry requirements.

In contrast, the adjoint vev,  $\sigma$ , leads to different contributions to  $Y_d$  and  $Y_e$ . Since  $\langle \Sigma_{24}(45_H) \rangle \propto Y$  and the (unnormalized) hypercharge generator is given by  $\sigma_2 \otimes \text{diag}(2, 2, 2, -3, -3)$ , we can group them into two different effective operators,  $h_1$  and  $h_2$ , such that

$$\begin{aligned} Y_d &= \frac{v_0}{M_{\text{Pl}}} Y_2 - 3 \frac{\sigma}{M_{\text{Pl}}} h_1 + 2 \frac{\sigma}{M_{\text{Pl}}} h_2, \\ Y_e^\top &= \frac{v_0}{M_{\text{Pl}}} Y_2 - 3 \frac{\sigma}{M_{\text{Pl}}} h_1 - 3 \frac{\sigma}{M_{\text{Pl}}} h_2. \end{aligned} \quad (141)$$

As a result, Eq. (1) will be modified. Hence, these operators with  $\langle \Sigma_{24}(45_H) \rangle$  can naturally explain

<sup>8</sup>Unfortunately, the authors of Ref. [12] do not specify how  $\text{SU}(5)$  is broken. They only mention the  $\text{SU}(5)$  singlet vev, which is necessary for the masses of down quark and charged lepton not to be too small. With the given Higgs fields, however,  $45_H$  has to break the  $\text{SU}(5)$  symmetry.

<sup>9</sup>Note that a second ten-dimensional Higgs field is required for a non-vanishing coupling  $10_H 45_H 10'_H$  in the superpotential. However, in order to have only two massless doublets, usually all components of  $10'_H$  become massive when the  $\text{SU}(5)$  symmetry is broken.

<sup>10</sup>In Ref. [35], Eqn. (29c) should read

$$\hat{Y}_{16} = \frac{h_{ij}^{16}}{M_{16}} \left\{ \frac{1}{4} \epsilon_{abcde} 10_i^{ab} 10_j^{cd} H^d \Sigma_f^e + \overline{H}_a \Sigma_b^a 10_i^{bc} 5_{jc}^* + \overline{H}_a 10_i^{ab} \Sigma_b^c 5_{jc}^* \right\}_A$$

such that  $h^{16}$  is antisymmetric. For a more substantiated approach to describe the vector-spinor 144, see Refs. [84].

the unsuccessful Yukawa unification for the lighter generations. Note that we only deal with one set of operators (140) so that they appear with both possible vevs of the adjoint Higgs field  $45_H$ .

## References

- [1] U. Amaldi, W. de Boer and H. Fürstenau, Phys. Lett. B **260**, 447 (1991).
- [2] J. C. Pati and A. Salam, Phys. Rev. D **8** (1973) 1240.
- [3] H. Georgi and S. L. Glashow, Phys. Rev. Lett. **32** (1974) 438.
- [4] H. Georgi, in: *Particles and fields* (ed. C. Carlson), AIP Conf. Proc. **23** (1975) 575; H. Fritzsch and P. Minkowski, Annals Phys. **93** (1975) 193.
- [5] H. Georgi and S. L. Glashow, Phys. Rev. D **6**, 429 (1972).
- [6] P. Minkowski, Phys. Lett. B **67**, 421 (1977).
- [7] G. D’Ambrosio, G. F. Giudice, G. Isidori and A. Strumia, Nucl. Phys. B **645** (2002) 155.
- [8] M. C. Gonzalez-Garcia and M. Maltoni, Phys. Rept. **460** (2008) 1.
- [9] S. Baek, T. Goto, Y. Okada and K. i. Okumura, Phys. Rev. D **63** (2001) 051701.
- [10] T. Moroi, JHEP **0003** (2000) 019; Phys. Lett. B **493** (2000) 366.
- [11] N. Akama, Y. Kiyo, S. Komine and T. Moroi, Phys. Rev. D **64** (2001) 095012.
- [12] D. Chang, A. Masiero and H. Murayama, Phys. Rev. D **67** (2003) 075013.
- [13] J. Hisano and Y. Shimizu, Phys. Lett. B **565** (2003) 183.
- [14] R. Barbieri, L. J. Hall and A. Strumia, Nucl. Phys. B **449** (1995) 437; Nucl. Phys. B **445** (1995) 219.
- [15] A. H. Chamseddine, R. Arnowitt and P. Nath, Phys. Rev. Lett. **49** (1982) 970; R. Barbieri, S. Ferrara and C. A. Savoy, Phys. Lett. B **119** (1982) 343.
- [16] J. R. Ellis, T. Falk, G. Ganis, K. A. Olive and M. Srednicki, Phys. Lett. B **510** (2001) 236 [arXiv:hep-ph/0102098].  
J. R. Ellis, D. V. Nanopoulos and K. A. Olive, Phys. Lett. B **508** (2001) 65 [arXiv:hep-ph/0102331].  
M. Battaglia *et al.*, in *Proc. of the APS/DPF/DPB Summer Study on the Future of Particle Physics (Snowmass 2001)* ed. N. Graf, *In the Proceedings of APS / DPF / DPB Summer Study on the Future of Particle Physics (Snowmass 2001), Snowmass, Colorado, 30 Jun - 21 Jul 2001, pp P347* [arXiv:hep-ph/0112013].
- [17] S. Bertolini, F. Borzumati, A. Masiero and G. Ridolfi, Nucl. Phys. B **353** (1991) 591.
- [18] R. Harnik, D. T. Larson, H. Murayama and A. Pierce, Phys. Rev. D **69** (2004) 094024.
- [19] A. L. Kagan, arXiv:hep-ph/0407076.
- [20] M. Endo, S. Mishima and M. Yamaguchi, Phys. Lett. B **609** (2005) 95 [arXiv:hep-ph/0409245].
- [21] D. T. Larson, H. Murayama and G. Perez, JHEP **0507** (2005) 057 [arXiv:hep-ph/0411178].
- [22] S. Jäger and U. Nierste, Eur. Phys. J. C **33** (2004) S256; arXiv:hep-ph/0410360, in: *Proceedings of 12th International Conference on Supersymmetry and Unification of Fundamental Interactions (SUSY2004), Tsukuba, Japan, June 17-23, 2004*, Eds. K. Hagiwara, J. Kanzaki, N. Okada. S. Jager, arXiv:hep-ph/0505243, in: *Proceedings of the XLth Rencontres de Moriond, Electroweak Interactions and Unified Theories, 5-12 March 2005, La Thuile, Italy*, Ed. J. Tran Thanh Van.
- [23] O. Tajima, 2005 Aspen winter conference, “Review on  $\sin(2\phi_1)$  and CPV in  $b \rightarrow s$  Decays”
- [24] A. Abulencia *et al.* [CDF Collaboration], Phys. Rev. Lett. **97** (2006) 242003.
- [25] T. Aaltonen *et al.* [CDF Collaboration], Phys. Rev. Lett. **100** (2008) 161802.
- [26] V. M. Abazov *et al.* [DØ Collaboration], Phys. Rev. Lett. **101** (2008) 241801. [arXiv:0802.2255 [hep-ex]].
- [27] T. Aaltonen *et al.* [CDF collaboration], CDF public note 10206.
- [28] V. M. Abazov *et al.* [DØ collaboration], DØ Conference note 6098.
- [29] V. M. Abazov *et al.* [DØ Collaboration], Phys. Rev. D **82** (2010) 032001 [arXiv:1005.2757 [hep-ex]].  
V. M. Abazov *et al.* [DØ Collaboration], Phys. Rev. Lett. **105** (2010) 081801 [arXiv:1007.0395 [hep-ex]].

- [30] CDF public note 9015 (2007).
- [31] W. Altmannshofer, A. J. Buras and P. Paradisi, Phys. Lett. B **669** (2008) 239 [arXiv:0808.0707 [hep-ph]].
- [32] E. Barberio *et al.* [Heavy Flavor Averaging Group], arXiv:0808.1297 [hep-ex].
- [33] The Heavy Flavor Averaging Group *et al.*, arXiv:1010.1589 [hep-ex].
- [34] S. M. Barr and S. Raby, Phys. Rev. Lett. **79** (1997) 4748 [arXiv:hep-ph/9705366]; K. S. Babu, J. C. Pati, Z. Tavartkiladze, JHEP **1006** (2010) 084. [arXiv:1003.2625 [hep-ph]].
- [35] S. Wiesenfeldt, Phys. Rev. D **71** (2005) 075006.
- [36] S. M. Barr and I. Dorsner, Phys. Lett. B **632** (2006) 527.
- [37] J. A. Casas, A. Ibarra and F. Jimenez-Alburquerque, JHEP **0704**, 064 (2007);  
J. Sayre and S. Wiesenfeldt, Phys. Rev. D **77** (2008) 053005.
- [38] S. Trine, S. Westhoff and S. Wiesenfeldt, JHEP **0908** (2009) 002 [arXiv:0904.0378 [hep-ph]].
- [39] J. Girrbach, S. Mertens, U. Nierste and S. Wiesenfeldt, JHEP **1005** (2010) 026 [arXiv:0910.2663 [hep-ph]].
- [40] J. Rosiek, arXiv:hep-ph/9511250.
- [41] M. Drees, Phys. Lett. B **181** (1986) 279;  
J. S. Hagelin and S. Kelley, Nucl. Phys. B **342** (1990) 95.
- [42] See, e.g., T. van Ritbergen, A. N. Schellekens and J. A. M. Vermaseren, Int. J. Mod. Phys. A **14** (1999) 41.
- [43] See also P. Nath and R. M. Syed, Phys. Lett. B **506** (2001) 68 [Erratum-ibid. B **508** (2001) 216]; P. Nath and R. M. Syed, Nucl. Phys. B **618** (2001) 138.
- [44] C. T. Hill, Phys. Rev. D **24** (1981) 691.
- [45] B. Pendleton and G. G. Ross, Phys. Lett. B **98** (1981) 291.
- [46] M. S. Carena, M. Olechowski, S. Pokorski and C. E. M. Wagner, Nucl. Phys. B **419** (1994) 213 [arXiv:hep-ph/9311222].
- [47] S. P. Martin and M. T. Vaughn, Phys. Rev. D **50** (1994) 2282.
- [48] D. M. Pierce, J. A. Bagger, K. T. Matchev and R. j. Zhang, Nucl. Phys. B **491**, 3 (1997) [arXiv:hep-ph/9606211].
- [49] J. Hisano and D. Nomura, Phys. Rev. D **59** (1999) 116005.
- [50] C. Amsler *et al.* [Particle Data Group], Phys. Lett. B **667**, 1 (2008).  
Nakamura *et al.* [Particle Data Group], J. Phys. G **G37** (2010) 075021.
- [51] K. Cheung, S. K. Kang, C. S. Kim and J. Lee, Phys. Lett. B **652** (2007) 319.
- [52] J. Hisano and Y. Shimizu, Phys. Lett. B **669** (2008) 301 [arXiv:0805.3327 [hep-ph]]. *for similar earlier studies see:* K. Cheung, S. K. Kang, C. S. Kim and J. Lee, Phys. Lett. B **652** (2007) 319 [arXiv:hep-ph/0702050]. T. Goto, Y. Okada, T. Shindou and M. Tanaka, Phys. Rev. D **77** (2008) 095010 [arXiv:0711.2935 [hep-ph]].
- [53] P. Ko, J. h. Park and M. Yamaguchi, JHEP **0811** (2008) 051 [arXiv:0809.2784 [hep-ph]]. J. h. Park and M. Yamaguchi, Phys. Lett. B **670** (2009) 356 [arXiv:0809.2614 [hep-ph]].
- [54] A. J. Buras, M. Nagai and P. Paradisi, arXiv:1011.4853 [hep-ph].
- [55] A. Lenz *et al.*, arXiv:1008.1593 [hep-ph], *to appear in* Phys. Rev. D.
- [56] A. J. Buras, M. Jamin and P. H. Weisz, Nucl. Phys. B **347**, 491 (1990).
- [57] A. J. Buras, P. Gambino, M. Gorbahn, S. Jäger and L. Silvestrini, Nucl. Phys. B **592** (2001) 55.
- [58] A. Lenz and U. Nierste, JHEP **0706** (2007) 072.
- [59] T. Besmer, C. Greub and T. Hurth, Nucl. Phys. B **609** (2001) 359.
- [60] F. Borzumati, C. Greub, T. Hurth and D. Wyler, Phys. Rev. D **62** (2000) 075005.
- [61] M. Misiak and M. Steinhauser, Nucl. Phys. B **764**, 62 (2007).
- [62] E. Barberio *et al.* [Heavy Flavor Averaging Group (HFAG)], arXiv:hep-ex/0603003.
- [63] K. Hayasaka *et al.* [Belle Collaboration], Phys. Lett. B **666** (2008) 16 [arXiv:0705.0650 [hep-ex]].
- [64] J. Benitez [BABAR Collaboration], arXiv:1006.0314 [hep-ex].
- [65] J. Hisano, T. Moroi, K. Tobe and M. Yamaguchi, Phys. Rev. D **53** (1996) 2442.

- [66] S. Jäger, “Supersymmetric SO(10) unification and flavor-changing weak decays,” PhD thesis, Techn. Univ. München, 2003.
- [67] S. Heinemeyer, Int. J. Mod. Phys. A **21** (2006) 2659 [arXiv:hep-ph/0407244].
- [68] R. Barate *et al.* [LEP Working Group for Higgs boson searches and ALEPH Collaboration and and], Phys. Lett. B **565** (2003) 61 [arXiv:hep-ex/0306033].
- [69] W. Martens, L. Mihaila, J. Salomon and M. Steinhauser, Phys. Rev. **D82** (2010) 095013. [arXiv:1008.3070 [hep-ph]].
- [70] T. Teubner, K. Hagiwara, R. Liao, A. D. Martin and D. Nomura, arXiv:1001.5401 [hep-ph].
- [71] S. Bethke, Eur. Phys. J. C **64** (2009) 689 [arXiv:0908.1135 [hep-ph]].
- [72] [CDF and DØ Collaborations], arXiv:1007.3178 [hep-ex].
- [73] K. G. Chetyrkin, J. H. Kuhn, A. Maier *et al.*, Phys. Rev. **D80** (2009) 074010. [arXiv:0907.2110 [hep-ph]].
- [74] K. G. Chetyrkin, J. H. Kuhn, M. Steinhauser, Comput. Phys. Commun. **133** (2000) 43-65. [hep-ph/0004189].
- [75] P. F. Harrison, D. H. Perkins and W. G. Scott, Phys. Lett. B **530** (2002) 167 [arXiv:hep-ph/0202074].
- [76] L. Wolfenstein, Phys. Rev. Lett. **51** (1983) 1945.
- [77] J. Charles *et al.* [CKMfitter Group], Eur. Phys. J. C **41** (2005) 1 [arXiv:hep-ph/0406184].
- [78] J. A. Casas, in *Perspectives on supersymmetry*, ed. G.L. Kane, World Scientific 1998, 378-401. [hep-ph/9707475]. J. A. Casas and S. Dimopoulos, Phys. Lett. B **387** (1996) 107 [arXiv:hep-ph/9606237].
- [79] B. Dutta and Y. Mimura, Phys. Rev. Lett. **97** (2006) 241802 [arXiv:hep-ph/0607147]. B. Dutta and Y. Mimura, Phys. Rev. D **75** (2007) 015006 [arXiv:hep-ph/0611268]. B. Dutta, Y. Mimura and Y. Santoso, Phys. Rev. D **82** (2010) 055017 [arXiv:1007.3696 [hep-ph]].
- [80] M. Ciuchini, A. Masiero, L. Silvestrini, S. K. Vempati and O. Vives, Phys. Rev. Lett. **92** (2004) 071801.
- [81] M. Albrecht, W. Altmannshofer, A. J. Buras, D. Guadagnoli and D. M. Straub, JHEP **0710** (2007) 055 [arXiv:0707.3954 [hep-ph]].
- [82] R. Dermisek and S. Raby, Phys. Lett. B **622** (2005) 327 [arXiv:hep-ph/0507045].
- [83] W. Altmannshofer, D. Guadagnoli, S. Raby and D. M. Straub, Phys. Lett. B **668** (2008) 385 [arXiv:0801.4363 [hep-ph]].
- [84] K. S. Babu, I. Gogoladze, P. Nath and R. M. Syed, Phys. Rev. D **72** (2005) 095011; Phys. Rev. D **74** (2006) 075004.